universität wien

# MASTERARBEIT | MASTER'S THESIS

Titel | Title

The effects of metal cations on dsRNA degradation at iron-oxide surfaces

verfasst von | submitted by

Sofie Marie Reiter B.Sc.

angestrebter akademischer Grad | in partial fulfilment of the requirements for the degree of

Master of Science (MSc)

Wien | Vienna, 2024

| | |
|---|---|
| Studienkennzahl lt. Studienblatt \| Degree programme code as it appears on the student record sheet: | UA 066 299 |
| Studienrichtung lt. Studienblatt \| Degree programme as it appears on the student record sheet: | Masterstudium Environmental Science |
| Betreut von \| Supervisor: | Univ.-Prof. Dipl.-Geol. Dr. Stephan Krämer |

## Acklowledgements

I want to express my deep gratitude to my advisors Prof. Stephan Krämer and Dr. Richard Kimber for their outstanding supervision of my project. I highly appreciate their valuable feedback and stimulating discussions, providing great help with upcoming problems and motivating me for this work.

Special thanks goes to our lab technician Herwig Lenitz, who made this whole project possible through his everyday support with measurements, orders, and so much more.

Furthermore, I am extremely greatful for the help from my lab colleagues, especially Veer and Anita, who were always there to support me, answer my many questions and give their advice in lab but also life questions.

Big thanks to the whole EDGE-Krämer group for creating such a kind and welcoming working environment and helping me progress professionally and personally.

Last but not least I want to thank my family and friends, especially my flat mates and my partner, for supporting me during this time and also providing welcoming distractions and comfort inbetween.

## Abstract

A newly developed biopesticide technology uses double-stranded (ds)RNA molecules for pest control. It is crucial for ecological risk assessment to understand the fate of these pesticides in soils with regard to mobility, stability, and bioavailability. As the common ironhydroxide goethite has been shown to abiotically hydrolyse dsRNA at the surface, this thesis investigates the effects of surface adsorbed divalent cations ($Mg^{2+}$ and $Ca^{2+}$) on dsRNA degradation by geothite, by first comparing the adsorption behaviour of dsRNA to a metal-loaded goethite surface at three different pH conditions (pH 5, 7, 9) and then assessing the degrees of degradation by goethite with and without metals at pH 7 and 9. $Mg^{2+}$ and $Ca^{2+}$ were expected to form cation bridges between negatively charged surface sites and the negatively charged phosphodiester backbone of dsRNA, increasing adsorption but also decreasing degradation by partially changing the dsRNA adsorption mechanism to goethite from inner-sphere complex formation to cation-bridging. Consistently, at pH 7 dsRNA degradation by goethite was more advanced than at pH 9, and both cations decreased the degree of adsorption with a stronger effect from $Ca^{2+}$. At pH 9, degradation appeared to be slow, even with metals at the goethite surface, although these metals, especially $Mg^{2+}$, significantly increased overall adsorption to goethite. TapeStation data revealed that for smaller fragment sizes, degradation seemed to slow down, raising the question of whether goethite causes degradation or rather fragmentation of dsRNA.

# Zusammenfassung

Eine neu entwickelte Biopestizid-Technologie verwendet doppelsträngige (ds)RNA-Moleküle zur Schädlingsbekämpfung. Ein Verständnis für das Verhalten dieser Pestizide im Boden in Bezug auf Mobilität, Stabilität und Bioverfügbarkeit ist entscheidend für die ökologische Risikobewertung. Da gezeigt wurde, dass das häufig vorkommende Eisenhydroxid Goethit dsRNA an der Oberfläche abiotisch hydrolysiert, untersucht diese Arbeit die Auswirkungen von an der Oberfläche adsorbierten zweiwertigen Kationen ($Mg^{2+}$ und $Ca^{2+}$) auf den Abbau von dsRNA durch Goethit. Zunächst wird das Adsorptionsverhalten von dsRNA auf einer metallbeladenen Goethit-Oberfläche bei drei verschiedenen pH-Werten (pH 5, 7, 9) verglichen, und anschließend der Abbaugrad von dsRNA durch Goethit mit und ohne Metalle bei pH 7 und 9 bewertet. Es wurde erwartet, dass $Mg^{2+}$ und $Ca^{2+}$ Kationenbrücken zwischen negativ geladenen Oberflächenstellen und dem negativ geladenen Phosphodiester-Rückgrat der dsRNA bilden, was die Adsorption erhöhen, aber auch den Abbau verringern würde, indem der Adsorptionsmechanismus von dsRNA zu Goethit teilweise von der Bildung innerer Sphärenkomplexe auf Kationenbrücken umgestellt wird. Bei pH 7 war der Abbau von dsRNA durch Goethit weiter fortgeschritten als bei pH 9 und beide Kationen verringerten das Ausmaß der Adsorption, wobei $Ca^{2+}$ einen stärkeren Effekt zeigte. Bei pH 9 schien der Abbau langsam zu verlaufen, selbst in Anwesenheit von Metallen auf der Goethit-Oberfläche, obwohl diese Metalle, insbesondere $Mg^{2+}$, die Gesamtsorption an Goethit signifikant erhöhten. TapeStation-Daten zeigten, dass der Abbau bei kleineren Fragmentgrößen langsamer zu verlaufen schien, was die Frage aufwarf, ob Goethit tatsächlich den Abbau oder eher die Fragmentierung von dsRNA verursacht.

# Contents

## List of Figures

# 1 Introduction

Nucleic acids, deoxyribonucleic acid (DNA) and ribonucleic acid (RNA), are ubiquitous molecules in the environment due to the central role they play in living organisms. RNA, in particular, is a versatile molecule involved in a variety of cellular biological pathways, from protein synthesis to gene regulation (Berg, Tymoczko, Gatto jr, & Stryer, 2018). Recently, RNA has also found novel applications in biotechnology, including the development of RNA-based pesticides (Bramlett, Plaetinck, & Maienfisch, 2020). Unlike DNA, which predominantly exists as a double-stranded molecule, RNA is typically single-stranded within cells (Berg et al., 2018). However, novel RNA pesticide applications use double-stranded RNA (dsRNA) (Bramlett et al., 2020). Double-stranded RNA also occurs naturally, for instance, as genetic material in some viruses (Collier et al., 2016).

DNA persistence and degradation in the environment have been widely studied due to diverse applications across fields, such as using environmental DNA for species monitoring in ecology (Olds et al., 2016) and studying human history through ancient DNA analysis (Pruvost et al., 2007). Recently, RNA, both single- and double-stranded, has also gained relevance in an environmental context. Research has focussed on monitoring RNA viruses such as SARS-CoV-2 (Ahmed et al., 2020), refining ecological species monitoring (Yates, Derry, & Cristescu, 2021), and developing new bio pesticide technologies utilizing double-stranded RNA (dsRNA) molecules for pest control (Bramlett et al., 2020)

During the ongoing SARS-CoV-2 pandemic, which began in 2020 and resulted in numerous deaths, it became essential to develop early warning systems for local corona virus outbreaks to promptly implement necessary interventions. Ahmed et al. (2020) attempted to estimate numbers of infected individuals within a specific area of Australia by extracting single-stranded virus RNA (V'kovski, Kratzel, Steiner, Stalder, & Thiel, 2021) from wastewater treatment plants. They utilized reverse transcriptase quantitative polymerase chain reaction (RT-qPCR) as a method to estimate viral RNA copy numbers from wastewater samples and calculate ongoing infections. These estimates were then compared to actual infections in the observed population. While the method shows potential for being used as an early warning system for SARS-CoV-2 outbreaks, further refinement of virus concentration methods is needed to achieve higher accuracy (Ahmed et al., 2020). As virus particles and RNAs can mainly be

extracted from sewage sludge particle surfaces (Balboa et al., 2021), understanding more about their adsorption and stability could help refining these methods.

Nucleic acids are also extensively studied in environmental samples from soils, sediments, air and aquatic environments for applications in palaeontology (ancient DNA) or ecology (environmental DNA) (Cristescu & Hebert, 2018; Willerslev, Hansen, & Poinar, 2004). Environmental DNA (eDNA) can be used to identify the presence of species in an ecosystem, providing a helpful, non-invasive method for monitoring, for example, endangered or invasive species, particularly in aquatic ecosystems (Biggs et al., 2015; Cristescu & Hebert, 2018; Thomsen & Willerslev, 2015). In recent years, studying environmental RNA (eRNA) has also emerged as a field of research, as the molecule is more stable in the environment than previously believed and environmental mRNA can persist for up to 72 h (Marshall, Vanderploeg, & Chaganti, 2021; Wood et al., 2020; Yates et al., 2021). As eRNA is linked to gene expression, it can provide valuable information exceeding mere species identification (Yates et al., 2021). Knowledge on ecosystem conditions, stress responses, organism health and also phenotypes can be derived from analysing eRNA, which increases resolution compared to eDNA (Yates et al., 2021).

With the global population expected to reach 9.7 billion people by 2050 (Desa, 2019), ensuring persistent food security is one of the major challenges humanity faces today. Pesticides play an important role in securing sufficient harvests to feed the world, making pesticide development and production a significant industry. The market for biopesticides, in particular, is experiencing rapid growth currently with a compound annual growth rate (CAGR) of 15.9 % compared to a CAGR of 3.1 % for the crop protection chemicals market and is projected to reach a market value of 13.9 billion USD by 2028 ("Biopesticides Market Research Report," 2023). Biopesticides are becoming more relevant as alternatives to chemical pesticides due to their anticipated smaller impact on the environment compared to chemical pesticides (Bramlett et al., 2020; Olson, 2015). The second generation of biopesticide technologies targeting insects involves the use of dsRNA for pest control (Baum et al., 2007; Parker & Sander, 2017). These nucleic acid molecules can be produced by genetically modified crops as plant incorporated protectants (PIPs) or applied topically to plants (Bramlett et al., 2020). The process behind this technology is called RNA interference (RNAi), which is a mechanism that can be found in all eukaryotic organisms for post transcriptional gene silencing (Hannon, 2002) that likely evolved in relation to virus defence (Obbard, Gordon, Buck, & Jiggins, 2009). In this process, dsRNA

is diced into 21 base pair long small interfering RNAs (siRNAs) (Filipowicz, 2005; Martinez, Patkaniowska, Urlaub, Lührmann, & Tuschl, 2002; Price & Gatehouse, 2008). One strand then forms an RNA-induced silencing complex (RISC) together with the Agronaute protein, which binds to homologous mRNA regions and initiates degradation (Martinez et al., 2002; Price & Gatehouse, 2008). This entire process can be used to target specific insect species when ingestion of dsRNA molecules triggers a systemic response within the organism leading to degradation of mRNA coding for a specific protein (Bramlett et al., 2020). The amplification step relies on the presence of an RNA-dependent RNA polymerase, which can produce new dsRNA through interaction with the RISC complex (Price & Gatehouse, 2008).

The use of dsRNA pesticides in agriculture inevitably leads to their introduction into soils. Concentrations of these pesticides in soils are estimated to be in the range of around 1 $ng_{dsRNA}/g_{soil}$ (Zhang et al., 2020). The dsRNA molecules used in these applications are reported to range in size from about 100 to 1000 base pairs (Baum et al., 2007; Bolognesi et al., 2012; Mitter et al., 2017; Zhang et al., 2020). Understanding how these molecules behave in the environment, including their stability, degradation, and adsorption to soil minerals, is critical for assessing their environmental risks and ensuring the safety of dsRNA-based pest control strategies (Parker & Sander, 2017).

### 1.1 Nucleic acids: DNA vs RNA

Nucleic acids, DNA and RNA, are macromolecules that hold genetic information in their base sequence. These linear polymers are composed of monomers known as nucleotides. The single nucleotides consist of a pentose sugar with a nitrogen heterocyclic base bound through β-glycosidic bonds and a phosphate group. In DNA, the sugar is deoxyribose, while in RNA, it is ribose. The base pairs found in DNA are guanine (G) paired with cytosine (C), and thymine (T) paired with adenine (A). In RNA thymine is replaced by uracil (U). Besides this difference to DNA, RNA has a hydroxyl group at the 2'-carbon atom, whereas DNA has a hydrogen atom in the same position, which makes RNA more susceptible to hydrolysis.

The single nucleotides in nucleic acids are linked through phosphodiester bonds where the 3'-hydroxylgroup of the sugar binds the 5'-phosphate group of the next nucleotide, forming a negatively charged backbone. In double-stranded nucleic acids, the two strands are antiparallel and bound to each other through hydrogen bonds formed between the complementary bases. The guanine and cytosine bond is stronger compared to the adenine and thymine bond because G-C pairs form three hydrogen bonds, whereas A-T and A-U pairs form only two hydrogen bonds. Typically, DNA is double-stranded, whereas RNA is single-stranded. However, there

are some exceptions where RNA is present in double-stranded form, like in specific viral RNA or in RNA pesticides (Bramlett et al., 2020; Collier et al., 2016). The two strands in DNA are coiled around each other in a clockwise direction to form a double helix with a diameter of 2 nm. Each coil consists of 10.4 base pairs and is repeated every 3.4 nm. Additional stability of the structure is achieved through van-der-Waals forces between the stacked bases, so-called stacking forces. This type of helix is called B-DNA-helix and is the most common shape of DNA molecules under physiological conditions. Double-stranded RNA on the other hand is usually found in canonical A-form, which is a broader (2.6 nm) and shorter helix shape with 11 base pairs per coil (Nicholson, 1996). It is less flexible compared to the B-form found in DNA and the more compact shape also influences the behaviour during gel electrophoreses as the smaller charge-to-mass ratio of dsRNA reduces mobility in the gel with respect to DNA (Nicholson, 1996). (Berg et al., 2018)

### 1.2 Fate of dsRNA in agricultural soils

To predict dsRNA pesticide mobility and persistence in the environment, it is crucial to understand its fate in soil systems. Other than dsDNA, ssRNA is known to be unstable and susceptible to hydrolysis due to the extra OH-group on the ribose sugar. The stability of dsRNA is less studied but recent research revealed a higher stability of dsRNA to alkaline hydrolysis and metal catalysed hydrolysis in solution due to its duplex structure compared to ssRNA (Chatterjee et al., 2022; Zhang, Hodge, Chatterjee, Moon, & Parker, 2021). DNA is known to persist in the environment for very long periods of time, almost up to a million years (Willerslev & Cooper, 2005), which leads to the assumption that dsRNA could also survive for environmentally relevant periods of time. This is why studying the mobility and persistence to understand the fate of dsRNA in soils is especially important for environmental risk assessment of the new pesticide technology. Parker et al. (2019) developed a method for tracing dsRNA adsorption and degradation in soil using 32-Phosphorous (32P)-radiolabeled dsRNA. This method is particularly valuable for studying dsRNA pesticides, as it allows quantification of very low concentrations (ng/g soil) of the polymer.

In their study, Parker et al. (2019) investigated the fate of dsRNA molecules in soil solutions (supernatant separated from most soil particles, with active microorganisms still in solution) and soil suspensions. After 24 h in soil solution, no intact dsRNA was found; however, a large amount of high molecular weight products (HMWPs) was present. This indicates microbial uptake of dsRNA and its utilization for biomolecule synthesis. When the soil solution was filtered or X-ray pre-irradiated before dsRNA addition, the formation of HMWPs by microbes

was significantly reduced. Nonetheless, no intact dsRNA was detected in solution after 24 h, likely due to degradation by extracellular hydrolases.

In soil suspensions, dsRNA adsorbs to mineral surfaces and is utilized by microorganisms. Soil properties, such as basal respiration rate and soil organic carbon content influence the uptake of 32P-labelled dsRNA by microbes. In soils with higher clay content, less dsRNA could be extracted from the mineral surface compared to soils with high sand content. Parker et al. (2019) also hypothesized that adsorption of dsRNA to soil particles helps protect the molecules from microbial and enzymatic degradation. Hydrolases likely adsorb to soil particles, inhibiting their degrading function.

In conclusion, the main processes that dsRNA undergoes in soils, are adsorption to particles, degradation in solution, and uptake and utilization by microorganisms. The adsorption of dsRNA to soil particles has been overlooked in past studies. For instance, Dubelman et al. (2014), suggested in their research on the fate of dsRNA in soils that 90 % of dsRNA added to agricultural soils seems to be degraded by microbes and enzymes within less than 35 hours. The degradation of dsRNA was quantified as loss from solution in this study, neglecting particle surface adsorption. However, understanding these processes, especially the protection of dsRNA by mineral surface adsorption, is essential for predicting the environmental fate of dsRNA pesticides and assessing their potential risks.

### 1.3 Nucleic acid – mineral interactions

The potential protection of dsRNA from enzymatic degradation by adsorption to mineral surfaces, which Parker et al. (2019) have suggested, has already been shown to exist for DNA (Aardema, Lorenz, & Krumbein, 1983; Blum, Lorenz, & Wackernagel, 1997; Lorenz & Wackernagel, 1987; Paget, Monrozier, & Simonet, 1992; Romanowski, Lorenz, & Wackernagel, 1991; Schmidt & Martinez, 2017). DNA rapidly binds to clay (Paget et al., 1992), sand (Lorenz & Wackernagel, 1987; Romanowski et al., 1991), or goethite surfaces (Schmidt & Martinez, 2017), for example, and can be protected from nucleases like DNase I when adsorbed to these mineral surfaces. The extent of adsorption and protection of DNA depends on the soil type, with different binding mechanisms identified between DNA and particle surfaces for various minerals (Saeki & Kunito, 2010; Schmidt & Martinez, 2017; Yu et al., 2013). Clay-rich soils generally have a high capacity to bind nucleic acids due to their great surface area and larger number of binding sites (Blum et al., 1997; Levy-Booth et al., 2007). When DNA molecules adsorb to montmorillonite, a common clay mineral in agricultural soils, the primary binding mechanism is electrostatic interaction between the positively charged clay

surface and negatively charged DNA phosphate backbone (P Cai, Huang, Zhang, & Chen, 2006). Next to electrostatic interactions, ligand-exchange, cation-bridges, and hydrogen bonding are binding mechanisms identified for DNA-clay surface interactions (Beall, Sowersby, Roberts, Robson, & Lewis, 2009; P Cai et al., 2006; Saeki & Kunito, 2010; Yu et al., 2013). For ligand-exchange, the phosphate in the backbone of DNA binds directly to the hydroxyl groups at the clay surface, forming inner-sphere complexes (Saeki & Kunito, 2010; Yu et al., 2013). Cation-bridges between negatively charged mineral surfaces and the DNA backbone can form in the presence of multivalent cations like $Mg^{2+}$ or $Ca^{2+}$. These cations act as bridges between the negatively charged phosphate groups in DNA molecules and negatively charged mineral surfaces and allow for adsorption despite repulsive charges. (Lorenz & Wackernagel, 1987; Paget et al., 1992; Romanowski et al., 1991) Additionally, cations can also screen repulsive charges of neighbouring DNA molecules or even intramolecularly, resulting in tighter packing of DNA molecules at the surface (Sodnikar, Parker, Stump, ThomasArrigo, & Sander, 2021). Multivalent cations even form bridges intermolecularly, also resulting in tighter packing and higher adsorption. (Nguyen & Chen, 2007; Sodnikar et al., 2021) For iron oxyhydroxides like goethite, inner-sphere complex formation has been identified as an important binding mechanism next to electrostatic interactions (Schmidt & Martinez, 2017). Similar to the process at the clay surface, the DNA backbone interacts with hydroxyl groups at the goethite surface leading to Fe-O-P bond formation. DNA structure is not affected when the molecules adsorb to the mineral surface, and B-form seems to be retained (Schmidt & Martinez, 2017). As can be derived from considering the dominant binding mechanisms of DNA to mineral surfaces, both pH and ionic strength exert a strong influence on adsorption. The surface charge of many minerals is pH dependent, with positively charged surfaces at a pH below the point of zero charge (PZC). It has been shown that adsorption of DNA to goethite, sand and montmorillonite decreases with increasing pH and increases with higher ionic strength (Lorenz & Wackernagel, 1987; Paget et al., 1992; Romanowski et al., 1991; Schmidt & Martinez, 2017). As already mentioned, cation concentration and their valency play an important role in DNA adsorption, as multivalent cations screen charges between and within molecules and make adsorption of DNA to negatively charged mineral surfaces possible via cation bridge formation. Since dsRNA molecules only slightly differ from DNA molecules, primarily by the presence of the 2'-OH group on the RNA sugar, Sodnikar et al. (2021) expected both nucleic acids to interact similarly with mineral surfaces. They hypothesized that as both dsRNA and DNA are polyelectrolytes, they should adsorb to surfaces according to polyelectrolyte adsorption theory. In these processes, electrostatic interactions and inner-sphere complex formation primarily

govern the adsorption mechanisms (Sodnikar et al., 2021). To test their hypothesis, Sodnikar et al. (2021) investigated the adsorption of dsRNA to the iron (oxyhydr)oxides goethite, lepidocrocite, and hematite, comparing it directly with DNA adsorption to these minerals. Their findings strongly suggest that dsRNA behaves similarly to DNA in terms of adsorption mechanisms and kinetics, with the phosphodiester backbone of dsRNA molecules mainly involved in adsorption rather than the base pairs. The presence of cations and solution pH also seem to dictate the extents of dsRNA adsorption to these minerals. At pH values ranging from moderately acidic to circumneutral, the affinity of dsRNA for these iron (oxyhydr)oxide-surfaces is high, similar to that of DNA.

Contrary to the stability and protection from enzymatic degradation observed for DNA at mineral surfaces (Paget et al., 1992; Schmidt & Martinez, 2017), Zhang et al. (2020) found that dsRNA concentrations at soil particle surfaces decreased even more rapidly than solution dsRNA concentrations. This decline in concentration could potentially indicate abiotic degradation pathways at the mineral-water interface or the occurrence of non-extractable dsRNA at the surface. To better understand the fate of dsRNA at mineral surfaces, Zhang et al. (2023) further investigated the processes dsRNA undergoes across different mineral surfaces.
Even though dsRNA is rather stable against alkaline hydrolysis and metal catalysed hydrolysis compared to single-stranded RNA (ssRNA) (Chatterjee et al., 2022; Zhang et al., 2021), it seems to be hydrolysed at the goethite-water interface at an environmentally relevant degradation rate, with a degradation half-life of 13 h (Zhang et al., 2023). DNA, on the other hand, is not being degraded by goethite, likely due to the missing 2'-hydroxyl group (Zhang et al., 2023).
Given that pH and ionic strength both are relevant parameters for dsRNA adsorption, they also have a strong effect on dsRNA degradation at the mineral surface. Degradation is highest at pH 7, whereas at pH 5 and pH 9 less degradation could be observed. When conditions are more acidic, the concentration of hydroxide ions, which might be involved in degradation, is lower in solution. At higher pH values, the goethite surface is negatively charged and less adsorption of dsRNA to the mineral surface occurs, which slows degradation. Although higher ionic strength increases adsorption, it decreases degradation at pH 7. The reason might be a more compact conformation at the mineral surface, where the dsRNA molecules interact with fewer binding sites, resulting in slower degradation. (Zhang et al., 2023)
Degradation at mineral-water interfaces can also be observed with other iron oxides, such as hematite, suggesting that iron atoms are involved in the degradation reaction. In contrast,

montmorillonite does not seem to degrade dsRNA as the nucleic acid molecules primarily adsorb to the surface via electrostatic interactions (Peng Cai et al., 2007), opposed to inner-sphere complex formation between dsRNA and the goethite surface. Although other minerals, like kaolinite or gibbsite, have the potential to coordinate the phosphate groups in the dsRNA backbone, they irreversibly adsorb a large fraction of added dsRNA, making potential degradation at their surface less relevant in the environment, as adsorbed molecules are most likely not bioavailable. (Zhang et al., 2023)

Regarding these findings, Zhang et al. (2023) suggested a potential mechanism for the degradation of dsRNA at the goethite surface. When phosphate groups are coordinated by surface iron atoms, electron density is being drawn away from the phosphorous atom, increasing the electrophilicity of the phosphorous. A nucleophilic attack on the P atom by oxyanions from deprotonated 2'-hydroxylgroups is then favoured, resulting in cleavage of the phosphodiester bonds. The findings that degradation is reduced at lower pH, that DNA remains stable at the goethite surface and that minerals like montmorillonite, which bind RNA solely through electrostatic interactions, do not cause RNA degradation, all support the proposed mechanism.

However, there are still knowledge gaps to be investigated further regarding the hydrolysis of dsRNA on mineral surfaces. Nucleotide composition of nucleic acids can be a factor influencing molecular stability. A poly(A:U) dsRNA for example denatured at a lower pH than synthesized dsRNA, likely due to the absence of guanine and cytosine base pairs, which form three hydrogen bonds compared to two hydrogen bonds between adenine and uracil (Cruz-León, Vázquez-Mayagoitia, Melchionna, Schwierz, & Fyta, 2018; Zhang et al., 2020). Whether this has an impact on the degradation by hydrolysis of the phosphodiester bonds is unclear.

Furthermore, size of nucleic acid molecules seems to be relevant for their adsorption behaviour and their stability in soil environments (Paget et al., 1992). Longer nucleic acid molecules tend to adapt a conformation of so-called train and loop segments at mineral surfaces where trains are sections of the molecule directly bound to the surface and loops are hanging freely (Hesselink, 1977; Paget et al., 1992; Romanowski et al., 1991). Shorter polymer fragments on the other hand have been proposed to rather lie flat on the mineral surface (Kronberg, Holmberg, & Lindman, 2014). These differences could potentially also affect hydrolysis catalysed by mineral surfaces.

Zhang et al. (2023) demonstrated that increased ionic strength can reduce the degradation rates of dsRNA by goethite. This occurs through charge screening of repulsive negative charges of phosphodiester backbones, resulting in more compact packing at the mineral surface (Sodnikar

et al., 2021). However, their study only examined the effects of the monovalent cation $Na^{+}$. Research on DNA and RNA has shown that multivalent cations, such as $Mg^{2+}$ and $Ca^{2+}$, can enhance adsorption by forming cation bridges between negatively charged sites of mineral surfaces and the nucleic acid backbone (Paget et al., 1992; Sodnikar et al., 2021). Since dsRNA degradation by iron oxides requires direct contact between surface iron atoms and dsRNA molecules (Zhang et al., 2023), the presence of multivalent cations could potentially decrease degradation at the goethite surface. This master's thesis aims to investigate this assumption.

### 1.4 Aim of research and hypotheses: Goethite-metal-dsRNA interactions

This master's thesis examines how the cations $Ca^{2+}$ and $Mg^{2+}$, when adsorbed to goethite, influence the degradation of dsRNA at the mineral-water interface by conducting a series of degradation experiments. Additionally, the adsorption kinetics of dsRNA to the common clay mineral montmorillonite, where no surface degradation is expected, are compared to the kinetics of dsRNA adsorption to goethite.

#### 1.4.1 Goethite

Goethite (α-FeOOH) is the most common iron hydroxide mineral in soils (Schwertmann & Cornell, 2000). As the needle-shaped $Fe^{3+}$-mineral is very stable, it can be found across various climate zones worldwide. Its widespread occurrence makes understanding dsRNA interactions with goethite surfaces particularly relevant for assessing the environmental risks associated with dsRNA pesticides. Iron oxides form from weathering of primary iron containing minerals, like biotite or magnetite for example, whereby $Fe^{2+}$ is oxidized to $Fe^{3+}$ in the presence of atmospheric oxygen. Octahedra are the structural elements of iron oxides. In goethite, these octahedra, with an iron atom in the centre surrounded by three $O^{2-}$ and three $OH^{-}$ ions, are linked together at the edges forming double-chains, which are then again linked via octahedra corners. (Blume et al., 2016)

#### 1.4.2 Montmorillonite

Montmorillonite is one of the most common smectite clay minerals (Carrado, 2000), which are layered aluminosilicates consisting of approximately 1 nm thick sheets stacked upon each other (Beall et al., 2009). Montmorillonite has a 2:1 structure, with sheets consisting of two layers of tetrahedral silica lattices surrounding an octahedral alumina layer (Beall & Powell, 2011; Beall

et al., 2009). These sheets are turbostratic, meaning their orientation relative to each other, when stacked, can vary (Beall & Powell, 2011). Water molecules are usually adsorbed between the sheets (Beall et al., 2009). Clay minerals like montmorillonite are known to have a high cation exchange capacity and large surface area per unit of mass, which is why their applications are widely studied (Beall et al., 2009; Carretero, 2002).

### 1.4.3 Calcium and Magnesium

Calcium ($Ca^{2+}$) and Magnesium ($Mg^{2+}$) are among the five most abundant cations found in soils and are important nutrients for plants (Hazelton, 2016). Their exchangeable concentrations in soils typically range from around 10 – 150 mM for calcium and 5 – 75 mM for magnesium (Hazelton, 2016). As these divalent cations are present in most soils, understanding how these divalent cations affect dsRNA stability on goethite surfaces is critical for the environmental risk assessment of dsRNA-based pesticides. Multivalent cations like calcium and magnesium can influence adsorption of nucleic acids to mineral surfaces (Paget et al., 1992; Sodnikar et al., 2021) and therefore potentially affect degradation of dsRNA by goethite by altering the mode of adsorption.

### 1.4.4 Research questions and hypotheses

Considering the significance of calcium and magnesium in soil environments, it is hypothesized in this thesis that multivalent cations such as $Mg^{2+}$ and $Ca^{2+}$ impact the degradation of dsRNA on goethite surfaces by modifying the adsorption mechanism. Specifically, these cations may change adsorption from inner-sphere complex formation to more electrostatic interactions, which could lead to reduced degradation rates.

The main research question addressed in this thesis is:

To what extent do the divalent cations $Mg^{2+}$ and $Ca^{2+}$ influence the degradation of dsRNA by goethite and is this impact significant enough to be relevant in the context of environmental risk assessment for dsRNA pesticides?

Three additional hypotheses were formulated for the research conducted in this thesis:

- Degradation of dsRNA by goethite will be evident in kinetics data and differ from montmorillonite kinetics, where no degradation is anticipated
- More degradation is expected with $Ca^{2+}$ compared to $Mg^{2+}$
- Degradation of smaller fragments is expected to be less than for larger fragments

By exploring these hypotheses, this thesis aims to provide insights into the role of common soil cations in the environmental stability and degradation of dsRNA-based pesticides, which is crucial for understanding their potential risks in agricultural settings.

# 2 Materials and Methods

## 2.1 Goethite synthesis and characterization

The iron-oxide goethite used in the experiments was synthesized using the Schwertmann and Cornell (2000) method for preparing goethite from an alkaline system. 100 mL of 1 M $Fe(NO_3)_3$ (99.0-101.0%, certified ACS, Merck) solution and 180 mL of 5 M KOH (Merck) solution were prepared by adding the salts to Milli-Q water while stirring. The KOH solution was then added to the stirred $Fe(NO_3)_3$ solution in a 2 L polyethylene flask where ferrihydrite precipitated immediately. The suspension was diluted up to 2 L with Milli-Q water and incubated at 70 °C for 62 h for goethite to form. The alkaline supernatant was then discarded, fresh Milli-Q water was added as a first washing step, and the mineral left to settle over two days. After decanting part of the supernatant, the slurry was dialyzed in dialysis tubes (Spectra/Por ® 7 MWCO 3500, pre-treated) with frequent water exchanges until the measured conductivity was below 2 µS/cm (~ 5 days). Subsequently, the goethite suspension was centrifuged (Eppendorf, 5430) (5 min, 7000 rcf), cooled at – 80 °C for 10 mins and then freeze dried (Rieger) over 5 days. As a last step, the goethite was roughly ground, put into an oven at 50 °C over night, and afterwards finely ground. The synthesis of goethite was confirmed by scanning the mineral with X-ray diffraction (XRD) (Rigaku MiniFlex) (Range 10-80 °, step width 0.02 °, speed 0.2 °/min). For further characterization a scanning electron microscope image (SEM, FEI, Inspect S50) was taken. The surface area was determined by BET-analysis (Quantachrome, Nova 2000e).

## 2.2 RNA stock and concentration check

### 2.2.1 Sterile working protocol

To prevent degradation of double-stranded ribonucleic acid (dsRNA), it is important to apply sterile working methods. For master stock and experimental stock preparations, all work was conducted under the laminar flow hood (Thermo Scientific, HERASAFE KS). The work surfaces were wiped with 70 % ethanol and the UV-cleaning function of the laminar flow hood was applied for 30 mins before use. All glassware was acid washed (5% $HNO_3$, 12 h), washed with detergent, cleaned with 70 % ethanol and put into the oven at 120 °C for at least 1 h. Buffers and solutions were first pH-adjusted, then autoclaved prior to use (121°C, 2 h).

### 2.2.2 RNA stock preparation

A polyadenylic-polyuridylic (Poly(A:U)) dsRNA was purchased from InvivoGen. 10 mg of lyophilized dsRNA were dissolved in 10 mL of sterile physiological water included in the kit by adding the water to the closed dsRNA container with a sterile syringe and needle, resulting in a stock concentration of approximately 1 mg/mL dsRNA. The stock was left to fully dissolve in the fridge overnight. For long time storage, the dsRNA stock was divided into aliquots in Protein LoBind tubes (Eppendorf) and stored in the freezer at -20 °C, where it is stable for up to one year according to the manufacturer.

### 2.2.3 dsRNA quantification and fragment length

In all experiments conducted for this thesis, dsRNA concentrations were quantified using the NanoQuant Plate with the Tecan Infinite Mono 200 PRO plate reader for ultraviolet (UV)-light absorbance spectroscopy at a wavelength of 260 nm. After blanking with the respective sample buffer and measuring the absorbance of a sample, the nucleic acid concentration is calculated according to the Beer-Lambert law (Equation I) according to the manual. (Nwokeoji, Kilby, Portwood, & Dickman, 2017)

(I) $$A = \varepsilon \cdot d \cdot C$$

with A = Absorbance, ε = molar extinction coefficient (μL $ng^{-1}$ $cm^{-1}$), c = concentration (ng $\mu L^{-1}$), d = path length (cm)

The pathlength of the NanoQuant Plate was 0.5 mm and an extinction coefficient (ε) of 0.02 μL $ng^{-1}$ $cm^{-1}$ was used for calculating dsRNA concentration (Sodnikar et al., 2021). Each sample was measured on four different positions on the NanoQuant Plate for all experiments. The standard deviation of the same solution measured multiple times was always less than 3 %.
As quality control, a ratio of UV-light absorbance at 280 and 260 nm was calculated for each measurement, as proteins in a sample absorb light at 280 nm. The 260/280 ratio should lie around 2.0 for RNA when indicating high purity. However, it is strongly dependent on the nucleotide composition of the nucleic acids measured (Lehninger, 1975; "NanoDrop One User Guide," 2016). Also, solution pH influences this ratio, with a lower value observed at acidic pH and a higher value at basic pH (Wilfinger, Mackey, & Chomczynski, 1997).

The dsRNA fragment size distribution was assessed with automated gel electrophoreses using the Agilent 4150 TapeStation. Electrophoreses is based on the principle of separating charged molecules of different sizes by applying an electric current in a gel. Separation of negatively charged nucleic acid fragments occurs, as smaller molecules migrate further in the porous gel matrix. This creates distinct bands in the gel, corresponding to different molecular sizes (Kurreck, Engels, & Lottspeich, 2022).

Since no specific tape for dsRNA size distribution analysis is available from Agilent, trial runs were conducted using various tapes including the ssRNA standard and high sensitivity, DNA1000, and DNA5000 tapes. Each tape types exhibited differing size distributions with peaks ranging from 200 to 1400 base pairs (bp) and inconsistent concentration determination. Ultimately, the High Sensitivity DNA5000 tape (Agilent Technologies) was selected for analysis of degradation products as this tape delivered the most distinct peaks.

### 2.3 dsRNA stability tests

#### 2.3.1 Fridge

To see whether the dsRNA stock is stable in the fridge (4-8 °C) without being degraded, concentrations were measured on the plate reader after 0 h, 6 h, 1 day, 2 days, 4 days and 7 days, and fragment length was determined with automated agarose gel-electrophoreses (Agilent TapeStation) after 0, 24, and 48 h. The stock was diluted 1:10 in buffer (3 mM BisTris (Sigma-Aldrich), 30 mM NaCl (certified ACS, Merck)) in 2 mL tubes (Eppendorf Protein LoBind) to a concentration of approximately 100 ng/µL for concentration measurement and diluted 1:2 for the TapeStation measurement using High-Sensitivity RNA tapes (Agilent Technologies). Eppendorf Protein LoBind tubes were used in all further experiments to prevent adsorption of dsRNA to the tube walls.

#### 2.3.2 Room Temperature – Shaking and no shaking

For testing dsRNA stability at room temperature, solutions of three different concentrations (5, 50, 100 ng/µL) were prepared as duplicates from the stock (1 mg/mL) in BisTris buffer (3 mM, 30 mM NaCl), with a final sample volume of 100 µL. Samples were put on the shaker (neoLab, RM-2M, setting C3, 15 rpm) and concentrations were measured after 0 (T0), 6, 24, and 48 h on the plate reader. Fragment size was determined for T0 and after 24 h using the TapeStation. As

a control, duplicates with a concentration of 50 ng/µL were left at room temperature without shaking. For verifying TapeStation results, the measurements were performed with both the regular RNA tapes and the High Sensitivity (HS) RNA tapes.

### 2.4 dsRNA stability with metals in solution (Ni, Cu, Mg)

As further experiments were going to investigate the interaction of dsRNA with a metal-loaded goethite surface, the stability of dsRNA with different metals (Cu, Ni, Mg) present in solution had to be ensured. Therefore, dsRNA-stock (1 mg/mL) was diluted to 100 ng/µL in BisTris-buffer (6 mM, 60 mM NaCl). To account for the high sodium chloride concentration and the absence of buffer in the dsRNA master stock (154 mM NaCl), the dilution buffer concentration was adjusted accordingly. This was done for all further experiments involving dsRNA in this thesis.

For the stability test, 250 µL of dsRNA solution (100 ng/µL, 6 mM BisTris, 60 mM NaCl, pH 7) were combined with 250 µL of the respective metal stocks (Cu, Ni, Mg) and samples were vortexed. For each metal, two experimental concentrations of 2 ppm and 10 ppm were selected which equals 32 µM and 158 µM for Cu, 35 µM and 170 µM for Ni and 82 µM and 412 µM for Mg. The metal stocks were diluted in Milli-Q from 1 mM stocks, prepared by adding the respective salts $CuCl_2$ * 2 $H_2O$ (Merck, certified ACS), $NiCl_2$ * 6 $H_2O$ (Merck, certified ACS), and $MgCl_2$ * 6 $H_2O$ (Merck, certified ACS) to Milli-Q water. The dsRNA and metal solutions with concentrations of 50 ng dsRNA/µL, 3 mM BisTris and 30 mM NaCl were put on a shaker (15 rpm, at room temperature, in the dark) and RNA concentrations of samples were measured after 0, 1, and 24 h on the plate reader. As a control, dsRNA was mixed with Milli-Q water. The pH of the samples was checked after the experiment.

### 2.5 Metal adsorption isotherms to goethite

Before the investigation of dsRNA adsorption behavior onto a metal-loaded goethite surface, metal adsorption isotherms on goethite were conducted to determine the optimal metal concentration for achieving full saturation of the mineral surface, while ensuring minimal residual metal ions remain in solution. For the experiment, goethite (4 mg/mL) was hydrated for 24 h in HEPES buffer (6 mM (Carl ROTH, ≥99.5 %), 60 mM NaCl), stirring at 300 rpm and metal solutions of various concentrations were prepared in Milli-Q water from $MgCl_2$ and $CaCl_2$ salts. Then the mineral suspension was ultrasonicated for 3 mins and 750 µL were combined with 750 µL of metal solution in 2 mL tubes (Eppendorf Protein LoBind) with

experimental metal concentrations of 5, 10, 30, 50, 100, 150, 250, 350, 700, and 1000 ppb and 2 mg/mL goethite. For even particle distribution, the shaker was set to 900 rpm when pipetting the goethite suspension. The experiment was conducted in duplicates and samples were shortly vortexed after mixing. Before the experiment, the pH of each sample was measured and adjusted to 7 with NaOH (Amresco, reagent grade) and HCl (Thermo Fisher Scientific, certified ACS Plus) when necessary. After 24 h of incubation on the shaker (15 rpm, at room temperature, in the dark), the samples were filtered (0.45 µm) and diluted in 1 % $HNO_3$ for analysis with inductively coupled plasma mass spectrometry (Q-ICP-MS, Agilent Technologies, 7700).

### 2.6 Goethite and RNA kinetics

Goethite was prepared in HEPES buffer (3 mM, 30 mM NaCl) with a concentration of 2 mg/mL goethite and hydrated for 24 h, stirring at 300 rpm. The experiment was conducted in 5 mL tubes (Eppendorf Protein LoBind) in triplicates by mixing 1 mL of mineral suspension with 1 mL dsRNA stock (100 ng/µL), freshly diluted in HEPES buffer (3 mM, 30 mM NaCl). Experimental initial concentrations were 1 mg/mL goethite and 50 ng/µL dsRNA. For even particle distribution when pipetting, the goethite suspension was ultrasonicated for 3 mins before use and then stirred at 900 rpm. After vortexing for a few seconds, the tubes were put on a shaker (15 rpm, room temperature, in the dark). Aliquots of 100 µL were taken at different timepoints (0, 5, 10, 30 min, 1, 2, 4, 6, 7, 24, 48, 72, 144, 168, 360 h) by shortly vortexing the samples before pipetting and then centrifuging the aliquots at 20000 rcf for 20 mins. To prevent resuspension of the mineral pellet, 20 µL of supernatant were taken off right after centrifuging and then RNA concentration was measured on the plate reader. After the last timepoint, the pH of the samples was measured.

### 2.7 Montmorillonite kinetics

As montmorillonite is a mineral known to stabilize dsRNA at the surface compared to dsRNA degradation by goethite (Zhang et al., 2023), adsorption kinetics of dsRNA to montmorillonite were conducted. To achieve a similar surface area to Zhang et al. (2023) for comparison, a mineral loading of 9 mg/mL was chosen for the experiment after a first trial run (see Appendix, Fig. A3). The montmorillonite (purchased from clay mineral society, Purdue University, USA) was pre-treated by saturating the surface with cations from NaCl. Therefore, 15 mg of mineral were mixed into 1 L of MilliQ water and the pH of the suspension adjusted to 9.5 with NaOH.

After ultrasonication (5 min, 35 kHz) and stirring (1 h, 200 rpm) for better particle dispersion, the suspension was centrifuged (5 min, 100 g). The supernatant was discarded to remove particles with a hydrodynamic diameter of <2 µm. This process was repeated several times until the suspension was free from these small particles. For saturating the mineral surface with $Na^+$, NaCl was added to a concentration of 1 M and the suspension was then mixed on the magnetic stirrer for 24 h at 300 rpm. Afterwards, the suspension was centrifuged for 1 h at 7000 g and the $Na^+$ addition was repeated twice to achieve saturation. For removing excess salt, the suspension was dialyzed (Dialysis membrane Spectra/Por ® 7 MWCO 3500) until a conductivity of <3 µS/cm was reached. Montmorillonite was then freeze-dried, ground, and stored at 2-8°C as a powder.

Two RNA concentrations of 30 and 40 ng/µL were chosen to optimize reaction rates. For the experiment, montmorillonite was hydrated in 3 mM HEPES buffer (30 mM NaCl) for 24 h while stirring at 300 rpm and ultrasonicated for 3 mins right before use. RNA stocks were freshly diluted (in 3 mM HEPES, 30 mM NaCl) and then mixed 1:1 with the mineral suspension to a volume of 1 mL in 2 mL tubes (Eppendorf Protein LoBind). The mineral suspension was stirred at 900 rpm during pipetting for even particle distribution. While the reactors were on the shaker (15 rpm, room temperature, in the dark), aliquots of 100 µL were taken at multiple timepoints (1 min, 0.5, 1, 2, 4, 27 h). Reactors were vortexed for several seconds before aliquots were taken. These samples were then centrifuged (20000 rcf, 40 mins), 20 µL of the supernatant were put into fresh tubes and RNA concentrations measured on the plate reader. After the experiment, pH values were measured.

### 2.8 dsRNA adsorption to a metal loaded goethite surface

To compare the adsorption behaviour of dsRNA to goethite with the adsorption of dsRNA to a metal loaded mineral surface across various pH conditions (5, 7, and 9), dsRNA was added to goethite suspensions with and without metals adsorbed to the surface. Therefore, 5 mL of 2 mg/mL goethite stock were prepared at pH 5 (3 mM Acetate, 30 mM NaCl), 7 (3 mM HEPES, 30 mM NaCl), and 9 (3 mM Sodium Tetraborate, 30 mM NaCl). For the metal loaded mineral suspensions, the goethite suspension was ultrasonicated for 3 mins, then 20 µM of the respective 100 mM metal stocks (prepared with $MgCl_2$ and $CaCl_2$ salts) in 1 mM HCl were added to achieve a metal concentration of 400 µM and left to hydrate (24 h, 300 rpm). As the goethite was hydrated in the respective buffers, the pH of the solution was stable throughout the experiment. The dsRNA stocks were prepared freshly in the respective buffers and their

concentrations validated on the plate reader before use. For the experiment, triplicates with 50 µL of dsRNA stocks combined with 50 µL of the different goethite suspensions were prepared in 2 mL tubes (Eppendorf Protein LoBind). Right before use, the goethite suspensions were ultrasonicated for 3 mins and put on the stir plate at 900 rpm for even particle dispersion when pipetting. The initial experimental concentrations were 5, 10, 20, 25, 30, 35, 40, 45, 50 ng/µL dsRNA, 1 mg/mL goethite and 200 µM metal. The metal concentrations were selected to ensure that all available surface sites were occupied while leaving residual metal ions in solution. After vortexing for a few seconds, the samples were being left to equilibrate for 2 h on the shaker at 15 rpm (room temperature, in the dark). Following centrifugation of the samples (20000 rcf, 20 mins), 20 µL of the supernatant were transferred into a fresh tube (Eppendorf Protein LoBind) to prevent mineral resuspension, and residual dsRNA concentrations were measured on the plate reader. The pH of samples was measured at the end of each experiment by combining the triplicates in one Eppendorf tube.

### 2.9 Challenges with new dsRNA batch

After purchasing a new batch of Poly(A:U) dsRNA from InvivoGen, plate reader concentration measurements at pH 5 started resulting in approximately 15 % lower concentrations than the manufacturer stated whereas measurements at pH 7 and 9 were as expected. Furthermore, 260/280 ratios at all pHs were higher than in the first batch. To exclude any buffer impurities or properties as potential causes, the measurements were repeated with fresh acetate buffer (3 mM, 30 mM NaCl) and with MES buffer (3 mM (Merck), 30 mM NaCl) at pH 5.2. After still showing the same concentration deviations, RNA stock was diluted in MES buffer with pH 5.5, 6.0, and 6.5. Only at pH 6.5 the measured stock concentration matched the expected value. An adsorption spectrum for pH 5 (3 mM Acetate, 30 mM NaCl) and pH 7 (3 mM HEPES, 30 mM NaCl) was taken for 100 ng/µL RNA (Varian, 50 Conc). The RNA was also washed using silica spin columns (QIAGEN, MinElute PCR Purification Kit) to see whether this procedure caused any change in 260/280 ratios. Due to these complications, no degradation experiments were performed at pH 5. The different behaviour of the two batches also caused restrictions for comparing degradation and adsorption data. To check for differences between the two batches, the adsorption experiment at pH 9 with no metals was repeated for comparison.

### 2.10 dsRNA degradation at a metal loaded goethite surface

To investigate the influence of adsorbed metals on dsRNA degradation by goethite, degradation experiments at pH 7 (HEPES) and pH 9 (Sodium Tetraborate) were performed. Due to the difficulties with concentration analysis at pH 5, this condition was excluded in further experiments. Goethite suspensions were prepared as previously for RNA adsorption experiments with a goethite concentration of 2 mg/mL. A dsRNA concentration of 20 ng/µL was chosen for the experiment based on previous adsorption experiments, which indicated that at pH 7 and this RNA concentration, nearly all binding sites on the mineral surface were occupied. The experimental metal concentrations for calcium and magnesium were 200 µM. As previously done for RNA adsorption experiments, goethite was incubated with metals in the respective buffers for 24 h before use. The incubation period of RNA with goethite was 20 h (on shaker at 15 rpm, room temperature, in the dark) to ensure significant degradation, with an estimated half-life of 13 h (Zhang et al., 2023). The experiment was conducted in triplicates with an experimental volume of 100 µL in 2 mL tubes (Eppendorf Potein LoBind). Reactors with goethite and no metal at the surface were also included in triplicates. Controls with RNA in both buffers were done in duplicates. After incubation, samples were centrifuged (5 mins, 21100 rcf) and 80 µL of supernatant exchanged with an extraction buffer (3 mM Sodium tetraborate, 100 mM NaCl, 12 mM Orthophosphate, pH 9). RNA was extracted from the mineral surface for a period of 24 h (on shaker at 15 rpm, room temperature, in the dark), adopted from Zhang et al. (2023). To ensure RNA stability in the extraction buffer, a control of only RNA in extraction buffer was included in duplicates. After extraction, all samples were centrifuged (20 mins, 20 000 rcf). Supernatant RNA concentrations were analysed on the plate reader and fragment size distribution determined, using the TapeStation.

The High Sensitivity D5000 tape was used for analysing the degree of degradation after 20 h of incubation with goethite. To quantify degradation and compare the various treatments, a size range between 500-2500 bp was classified as *intact* RNA. All fragments between 100-500 bp were seen as *degraded*. The area under the curve was taken as a measure of relative concentration of these size pools within a sample. Degradation (D) was then quantified using a ratio of *intact* and *degraded* concentration (c) (Equation II). When using this equation, a higher value of D corresponds to a higher level of degradation of the initial dsRNA. The method was adapted from Zhang et al. (2023)

$$\text{(II)} \qquad D = \frac{\mathrm{c[RNA}\ degraded]}{\mathrm{c[RNA}\ intact]}$$

# 3 Results and Discussion

## 3.1 Goethite characterization

BET surface area analysis of goethite delivered a value of 37 $m^2/g$.

After synthesis, goethite was characterized by XRD analysis. The XRD-pattern, confirming the successful synthesis process is shown in Fig. 1.

An SEM image of goethite was taken at 5000x magnification to closely examine the mineral surface (Fig. 2). The scan clearly shows the needle-shaped particles, which are characteristic of goethite.

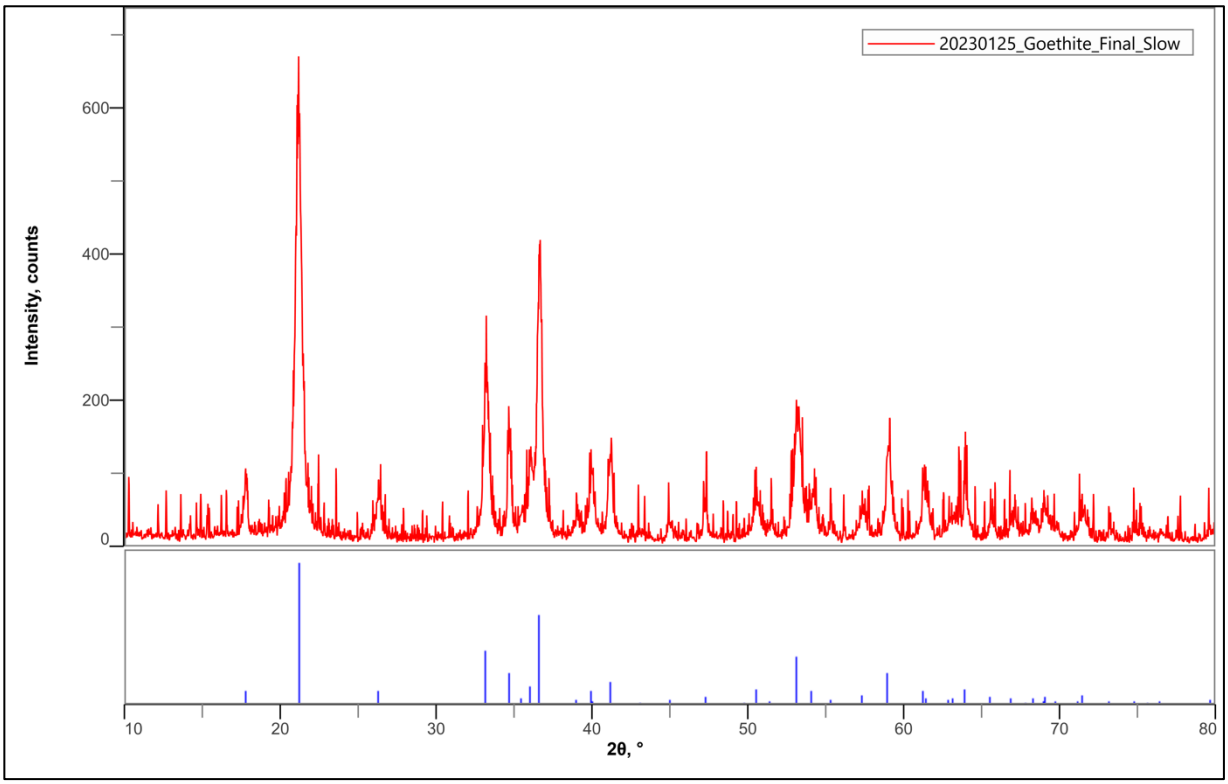


*Figure 1: Results from the XRD scan of the synthesized goethite (red) with peak positions of goethite from the data base (blue). The measurement was conducted with a range of 10-80 °, a step width of 0.02 °, and a speed of 0.2 °/min .*

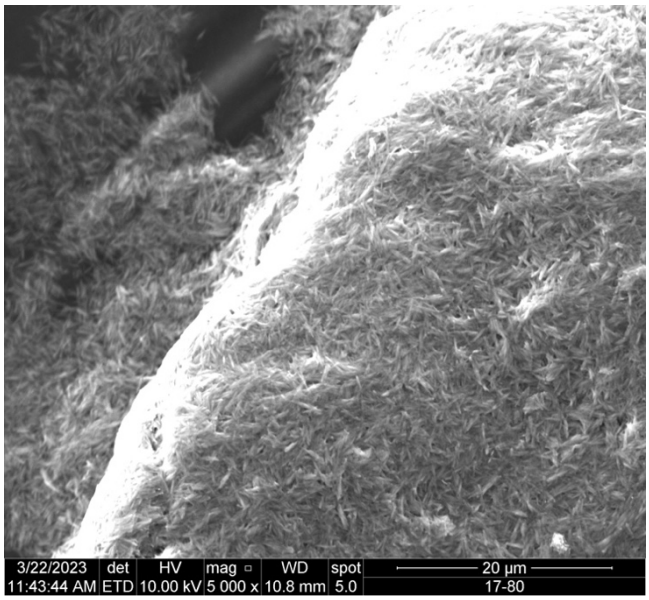


*Figure 2: SEM image of goethite (5000x magnification)*

### 3.2 dsRNA stability tests

Stability test results of dsRNA in the fridge (Fig. 3), at room temperature with (Fig. 5) and without shaking (Fig. 5) showed constant concentrations over 7 days or 48 h respectively, indicating that the nucleic acid molecules are stable under these conditions, which is also supported by the TapeStation results (Fig. 4). The peak positions correspond to fragment size and as the peaks overlapped for all three time points, the stability of dsRNA over 48 h in the fridge could be confirmed and no degradation was detected. The tapes used for analysis are not designed for dsRNA but rather for ssRNA, which is why peak hights often differed between two measurements of the same concentration and hence concentration could not be accurately measured or confirmed on the TapeStation.

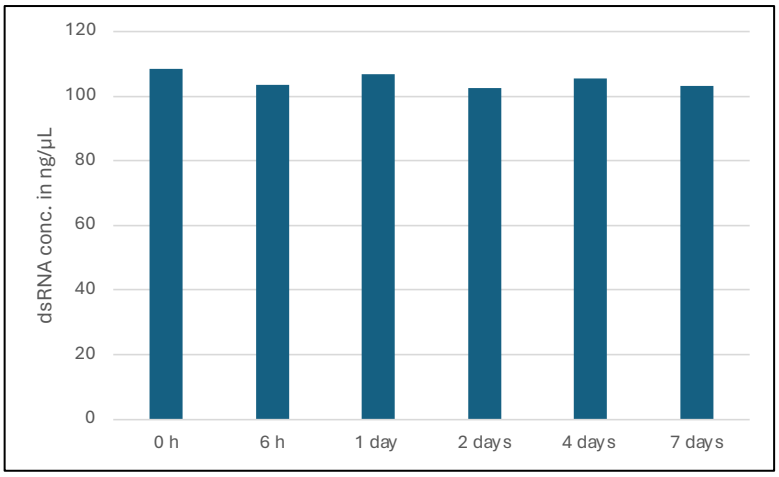


*Figure 3: Stability test of dsRNA stock (100 ng/µL RNA, 3 mM BisTris, 30 mM NaCl, pH 7) stored in the fridge. RNA concentrations of the solution were measured after 0 h, 6 h, 24 h, 2 days, 4 days, and 7 days on the plate reader.*

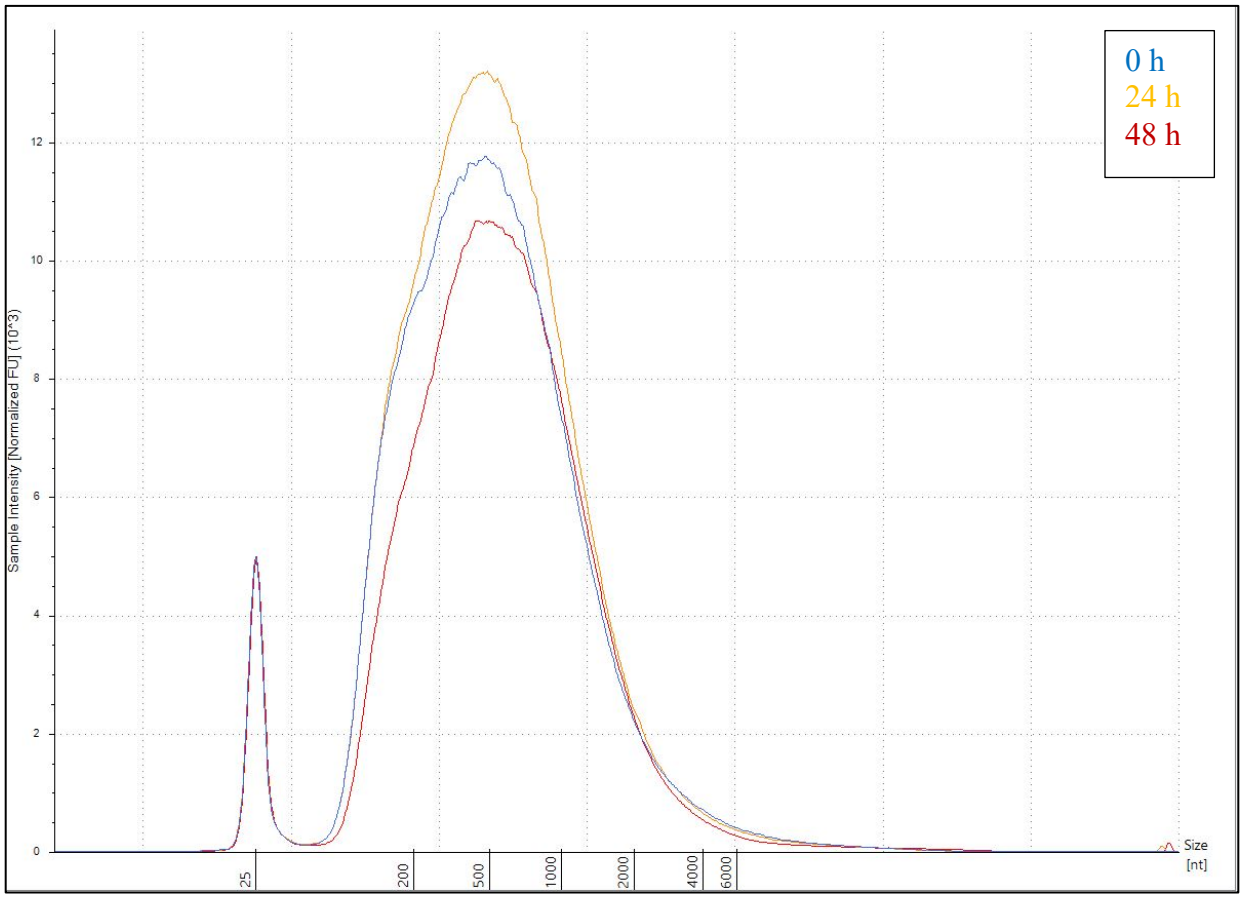


*Figure 4:Fragment size distribution of dsRNA stock (100 ng/µL 3 mM BisTris, 30 mM NaCl, pH 7) kept in the fridge and measured on the TapeStation after 0 h (blue), 24 h (orange), and 48 h (red) using the High-Sensitivity RNA screentape.*

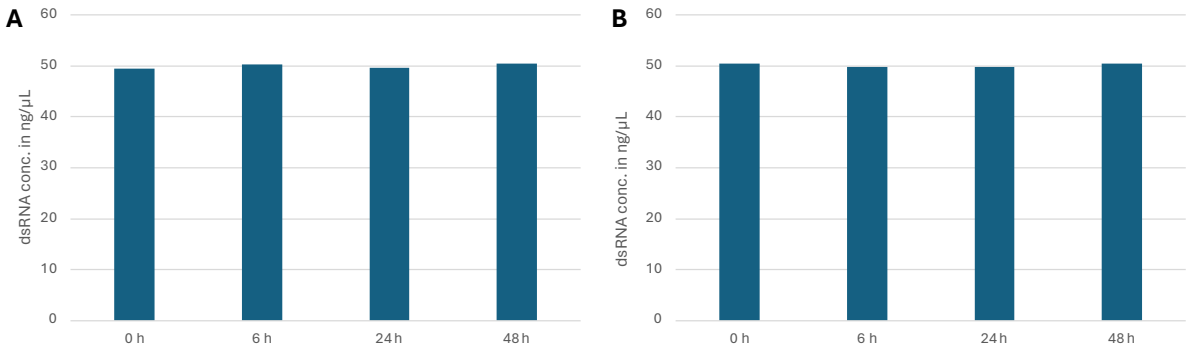


*Figure 5: Stability test of dsRNA in buffer (3 mM BisTris, 30 mM NaCl, pH 7) stored at room temperature without shaking (A) and while shaking at 15 rpm (B). RNA concentrations of the 50 ng/µL solution were measured after 0 h, 6 h, 24 h, and 48 h on the plate reader.*

### 3.3 dsRNA and metals in solution (Cu, Mg, Ni)

The stability of dsRNA in the presence of metal cations $Ni^{2+}$, $Cu^{2+}$, and $Mg^{2+}$ in solution was assessed to rule out any potential degrading effects of free metal ions on dsRNA during subsequent degradation experiments with metal-saturated goethite. Certain metals, such as copper, can act as Lewis acids and catalyse the hydrolysis of ssRNA, whereas dsRNA was proven to be rather stable against metal-catalysed hydrolysis (Chatterjee et al., 2022). Potential dsRNA degradation would be indicated by an increase in concentrations measured on the plate reader, as the degradation products of nucleic acids typically have higher absorbance (Nwokeoji et al., 2017). The results shown in Fig. 6 indicate, that there was no significant change in dsRNA concentration over a period of 24 h in the presence of all three metals at two different concentrations (32 µM and 158 µM for Cu, 35 µM and 170 µM for Ni and 82 µM and 412 µM for Mg). These findings align with the observations of Chatterjee et al. (2022) on dsRNA being relatively stable in the presence of metals. In contrast to ssRNA, dsRNA appears to be stable against metal-catalysed hydrolysis.

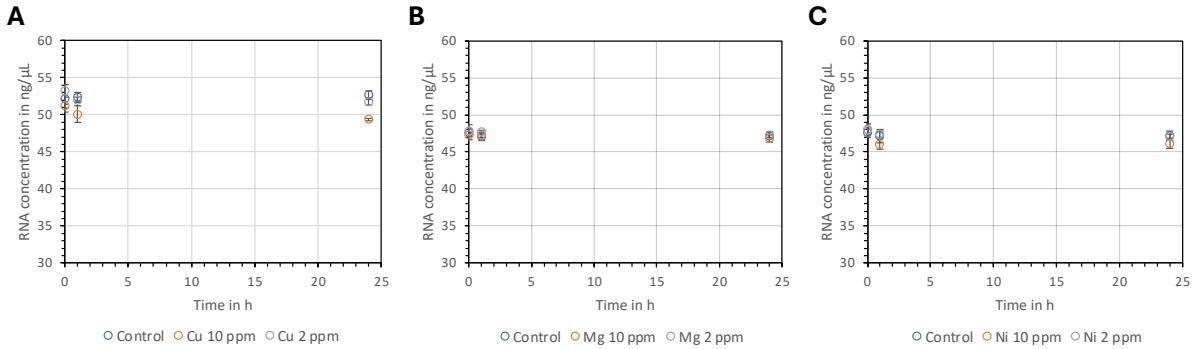


*Figure 6: RNA (50 ng/µL) in buffer solutions (3 mM BisTris, 30 mM NaCl, pH 7) with two different concentrations (2 ppm, 10 ppm) of copper (A), magnesium (B), and nickel (C). A control without metal was included. Sample concentrations were measured after 0, 1, and 24 h on the plate reader. The pH of all samples stayed stable at 7.1 over the course of the experiment.*

### 3.4 Metal adsorption isotherms to goethite

To confirm that $Mg^{2+}$ and $Ca^{2+}$ adsorb to the surface and to determine suitable experimental concentrations for saturating the mineral surface with metal ions, metal adsorption isotherms to goethite were conducted (Fig. 7). The adsorption capacity of magnesium was approximately ten times smaller compared to calcium. There were significant uncertainties in the data, partly due to high background concentrations of magnesium and calcium in the ICP-MS measurement, which made it challenging to detect the small differences between the initial metal

concentrations and the supernatant concentrations, especially for magnesium. In the literature, the reported amount of adsorbed magnesium ($Mg^{2+}$) to goethite at pH 7 is approximately 0.15 nmol/cm² for an initial magnesium concentration of 200 µM, with a goethite concentration of 3 mg/mL (Atouei, Rahnemaie, Kalanpa, & Davoodi, 2016). For calcium, the measured values matched the order of magnitude found in literature (Atouei et al., 2016). This means, the pronounced difference in calcium and magnesium adsorption to goethite is likely due to mistakes in the experiment, which should be repeated with stocks made in acidic buffer solution rather than water to prevent potential precipitation and to receive more reliable adsorption data.

For dsRNA adsorption and degradation experiments, a concentration of 200 µM $CaCl_2$ and $MgCl_2$ was chosen for both metals. This concentration was selected based on the isotherm data, aiming to find a point where the adsorbed metal concentration begins to plateau. The goal was to saturate the goethite surface as much as possible while minimizing the amount of metal remaining in solution.

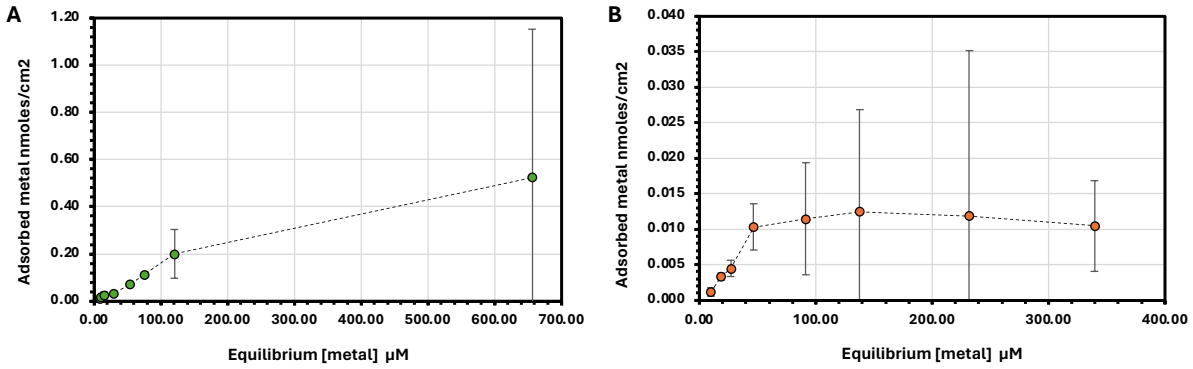


*Figure 7: Concentration-dependent adsorption of $Ca^{2+}$ (A) and $Mg^{2+}$ (B) to goethite (2 mg/mL) at pH 7 (3 mM HEPES, 30 mM NaCl) after incubation for 24 h. The pH stayed stable during the experiment.*

### 3.5 Goethite and dsRNA kinetics

Kinetic experiments of dsRNA adsorption were conducted in order to receive a good estimate for adsorption equilibration times in following adsorption experiments. Concentrations of 50 ng/µL of dsRNA and 1 mg/mL goethite were selected after trial runs (see Appendix, Fig. A1 and A2) as the amount of added RNA had to exceed the adsorption capacity of the mineral load to observe saturation. Rapid adsorption of a large fraction of dsRNA to goethite occurred within minutes (Fig. 8). These findings align with previous studies on DNA and RNA adsorption to goethite (Peng Cai, Huang, & Zhang, 2006; Sodnikar et al., 2021; Zhang et al.,

2020). In the beginning there is a strong gradient between high solution dsRNA concentration and no dsRNA at the goethite surface, resulting in fast diffusion towards the surface, where dsRNA is expected to be readily bound through electrostatic interactions and inner-sphere complex formation (Kronberg et al., 2014; Sodnikar et al., 2021). Below the PZC of approximately 7.5-7.9 (Cristiano, Hu, Sigfried, Kaplan, & Nitsche, 2011; Müller & Sigg, 1992), goethite is net positively charged, creating electrostatic attraction between negatively charged dsRNA molecules and the surface.

As measured UV-absorbance of the supernatant solution continued to decrease, it appeared that adsorbed concentrations increased to approximately 115 ng/cm$^2$ goethite for three more days and began to decrease again after 7 days. Opposed to DNA kinetics of adsorption to goethite (Sodnikar et al., 2021), no real equilibrium was expected to be reached, as dsRNA is known to hydrolyse at the surface (Zhang et al., 2023). The apparent continuous increase in dsRNA adsorption over several days likely indicated slow kinetics. As the experiment was conducted at pH 7, which is below the PZC of goethite, the mineral surface was expected to only carry a weak positive net charge (Antelo, Avena, Fiol, López, & Arce, 2005), which allows goethite particles to form aggregates due to weaker repulsive forces between particles (Xu, Deng, Li, & Xu, 2015). These aggregates may cause size exclusion of larger fragments as they might diffuse more slowly into the pore space of the mineral surface (Ogram, Mathot, Harsh, Boyle, & Pettigrew Jr, 1994). The Poly(A:U) dsRNA used in these experiments is known to consist of fragments between approximately 100-1000 bp (Zhang et al., 2020). In general, polydisperse mixtures of polymers take longer to equilibrate than monodisperse, as there is an exchange of low molecular weight species for high molecular weight species at the mineral surface (Kronberg et al., 2014; Terada, Samoshina, Nylander, & Lindman, 2004). Small dsRNA fragments adsorb to the surface first (Kronberg et al., 2014). However, the sudden steeper slope between 7 h and 24 h indicating a faster increase in adsorbed concentrations is difficult to explain with slower kinetics only. Simultaneous hydrolysis at the goethite surface likely exerted an influence on the observed behaviour but is hard to interpret without further information.

The decrease of adsorbed dsRNA after 7 days could be an indicator for hydrolysis at the surface. Some hydrolysis products including single-stranded RNA fragments and single nucleotides might end up in solution together with non-adsorbed intact dsRNA. The absorbance of hydrolysis products at 260 nm is higher than that of dsRNA, which alters concentration measurements on the plate reader (Nwokeoji et al., 2017). The increase of supernatant concentrations due to this higher absorbance, could lead to assuming a smaller amount of RNA at the mineral surface, reflected in the decline in Fig. 8. However, the generation of these

nucleoside monophosphates (NMPs) is very slow. Zhang et al. (2023) were able to extract only 30 % of the ssRNA added as NMPs after 190 days of incubation and for dsRNA this proportion was even less. This is why an additional explanation for decreasing dsRNA adsorption after 7 days could be required. The rearrangement of polymers at the surface potentially could also play a role in decreasing adsorption capacities, as they could start to lay flatter on the surface, occupying more binding sites (Kronberg et al., 2014).

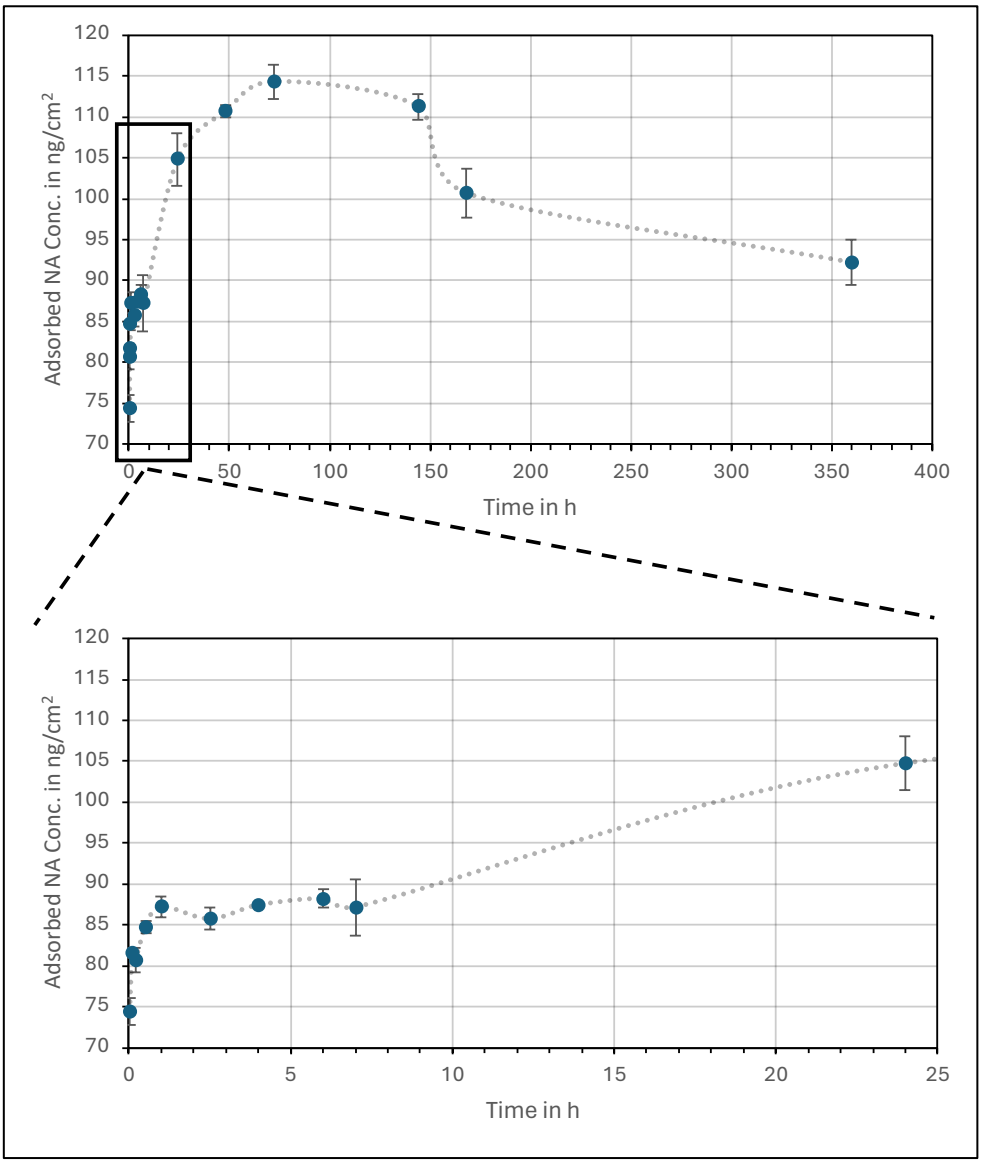


*Figure 8: Adsorption kinetics of dsRNA (initial concentration of 50 ng/µL) to goethite (1 mg/mL) at pH 7 (3 mM HEPES, 30 mM NaCl), determined by the decrease of dsRNA concentrations in the supernatant. The pH of the reactors stayed constant over the experiment.*

### 3.6 Montmorillonite kinetics

Kinetics of dsRNA adsorption to the clay mineral montmorillonite were conducted as a comparison to goethite kinetics (Fig 9). At pH 7, adsorption of dsRNA to montmorillonite is mainly driven by electrostatic interactions, and thus dsRNA is not expected to undergo surface catalysed hydrolysis (Zhang et al., 2023). Two dsRNA concentrations were selected to determine an optimal RNA-to-mineral ratio that would provide clear kinetics data. Surface adsorption was rapid within the first minutes, similar to the initial adsorption kinetics observed with goethite. After 27 h, the adsorbed nucleic acid concentrations reached approximately 6.1 ng/cm$^2$ for the 40 ng/µL dsRNA solution and 5.4 ng/cm$^2$ for the 30 ng/µL solution. Adsorption continued to increase for both concentrations between 5 and 27 h. The slow adsorption kinetics observed during this period may be due to the longer equilibration time of different size fragments of dsRNA between the adsorbed and solution phases, similar to the behaviour seen in goethite adsorption kinetics. Overall, montmorillonite exhibited a smaller adsorption capacity for dsRNA than goethite

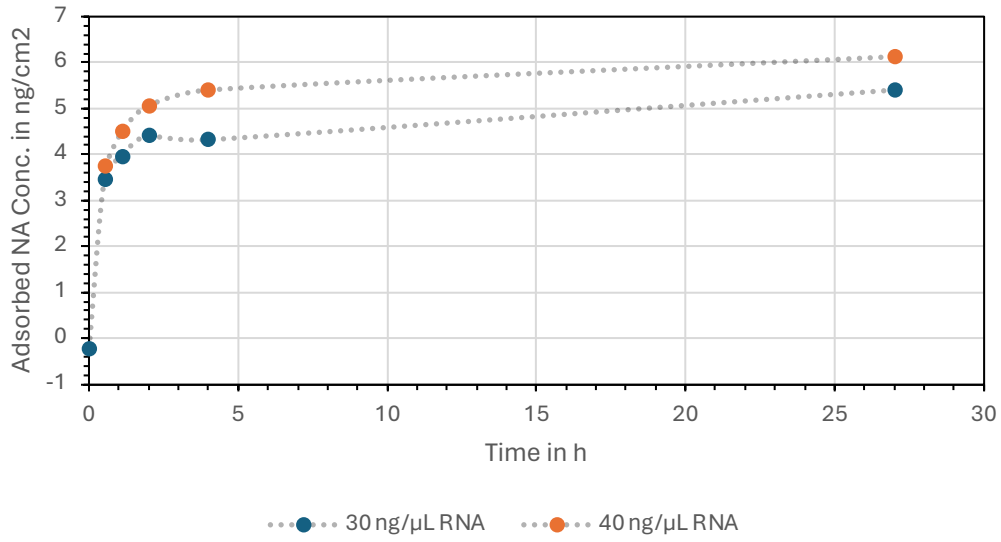


*Figure 9: Adsorption kinetics of montmorillonite and dsRNA with 9 mg/mL montmorillonite (3 mM HEPES, 30 mM NaCl) and two different initial RNA concentrations of 30 ng/µL (blue) and 40 ng/µL (orange). The solution pH was adjusted to 7 and stayed stable during the experiment.*

### 3.7 dsRNA adsorption to a metal saturated goethite surface

Adsorption experiments of dsRNA to goethite with calcium and magnesium ions pre-adsorbed to the mineral surface were conducted in order to evaluate to what extent these metals influence

adsorption behaviour. The experiments basically follow methods for adsorption isotherms, however, the term “isotherm” was avoided here as no real equilibrium was expected to be reached with simultaneous hydrolysis at the surface.

Although previous experiments showed that kinetics of dsRNA adsorption were slow after the first hour and adsorbed concentrations continued to increase for approximately 3 days (Fig. 10), an incubation time of 2 h was selected for these adsorption experiments. The reason for selecting a shorter incubation time is progressing degradation at the surface. Using rate constants for degradation kinetics determined by Zhang et al. (2023), 2 h where selected as an equilibration period where more than 90 % of initial dsRNA is still intact. Adsorption kinetics data also confirmed that there was no significant increase in adsorption between 2 and 7 h (Fig. 10). Overall, approximately 25 % of total potential adsorption capacity seem to be lost with shorter incubation times, under the assumption that maximum adsorption was only a result of slow kinetics and degradation is not influencing these values.

When no metals were present at the surface, adsorption was only influenced by pH. Highest adsorption was expected at pH 5, decreasing with increasing pH values. This corresponds to the data presented in Fig. 10 A-C. At pH 5, adsorption was highest with an adsorption capacity of approximately 100 ng/cm$^2$, followed by 80 ng/cm$^2$ at pH 7 and around 20 ng/cm$^2$ at pH 9. At pH 5 the goethite surface has a high positive net surface charge (Antelo et al., 2005), leading to strong electrostatic attraction between the negatively charged dsRNA backbone and positively charged mineral surface. At pH 7, the surface remains positively charged but weaker, as this pH value is closer to the PZC (Antelo et al., 2005), which is around 7.5-7.9. Above the PZC, the surface is negatively charged, resulting in electrostatic repulsion between dsRNA and goethite (Sodnikar et al., 2021), which is reflected in the data obtained at pH 9. Additionally, inner-sphere complex formation is expected to become less favourable with increasing pH (Sodnikar et al., 2021).

Calcium and magnesium cations were expected to increase the adsorption capacities of goethite for dsRNA molecules, and this hypothesis was confirmed by the experimental data. An increase in adsorption of dsRNA could be observed across all pH conditions for both cations. However, the extent of this increase was strongly pH dependent. At pH 5, adsorption capacities were increased by approximately 30 % with $Ca^{2+}$ and 20% with $Mg^{2+}$. The adsorption data suggests that adsorption capacities could reach even higher levels if additional data points with higher

dsRNA concentrations were included. This assumption is supported by the fact that the adsorbed dsRNA concentrations had not yet plateaued, as indicated in Fig. 10A. The trend implies that with increasing dsRNA concentrations, the goethite surface could continue to adsorb more dsRNA until saturation is eventually reached. It was anticipated that $Ca^{2+}$ would have a stronger effect on adsorption compared to $Mg^{2+}$, which could be confirmed for conditions at pH 5 and 7. $Ca^{2+}$ is the only alkaline earth metal known to form inner-sphere complexes with DNA, resulting in stronger bridges between nucleic acid molecules and mineral surfaces, whereas $Mg^{2+}$ forms outer-sphere complexes with DNA (Nguyen & Chen, 2007). It is assumed here, that this might also apply to dsRNA adsorption with calcium and magnesium ions. Furthermore, goethite exhibited a 10 times higher adsorption capacity for $Ca^{2+}$ compared to magnesium at pH 7 in previous metal adsorption isotherms (Fig. 7). However, this should not fully be taken into account, as comparison with literature data suggested smaller differences in adsorption behaviour to goethite for the two metals (Atouei et al., 2016). Magnesium has a stronger hydration shell compared to calcium (Nguyen, Chen, & Elimelech, 2010) and is more soluble in water (Paget et al., 1992), which might have resulted in less adsorption to goethite or RNA. Calcium ions form more stable bonds with the mineral surface and nucleic acid molecules, resulting in better bridging abilities (Nguyen & Chen, 2007).

At pH 7, $Ca^{2+}$ increased the capacity of goethite for dsRNA adsorption by approximately 45 % and $Mg^{2+}$ by 38 % (Fig. 10B). However, for the $Ca^{2+}$ data, the adsorpion plateau seemed to not have been reached yet. The stronger effect of divalent cations on adsorption at pH 7 compared to pH 5 was likely caused by more negative charges on the goethite surface, as this pH condition is closer to the PZC (Atouei et al., 2016). Diffusion of dsRNA towards the goethite surface is still favoured under these conditions as the net surface charge is positive. Cations can bridge more negative surface charges, likely causing the stronger effect on adsorption capacities. The difference between the two cations was less pronounced at pH 7.

At pH 9, the trend was reversed and magnesium exhibited a stronger effect on adsorption than calcium (Fig. 10C). Magnesium increased the adsorption capacity by approximately 150 % compared to 40 % observed for calcium. The surface was net negatively charged under these pH conditions, which likely made adsorption of dsRNA to the mineral surface unfavourable. Hence, cation bridging could have a strong effect on adsorption capacities, which was observed for magnesium. In comparison to magnesium, the effect of calcium on adsorption capacities was significantly lower, which is especially noticeable as higher bridging potential was

expected for calcium. However, calcium tends to form colloids and surface precipitates at pH 9 under the given conditions and metal concentrations (modelled with PhreeqC), likely diminishing its ability to form bridges between goethite and RNA and changing the entire system. Magnesium is expected to stay in solution at pH 9.

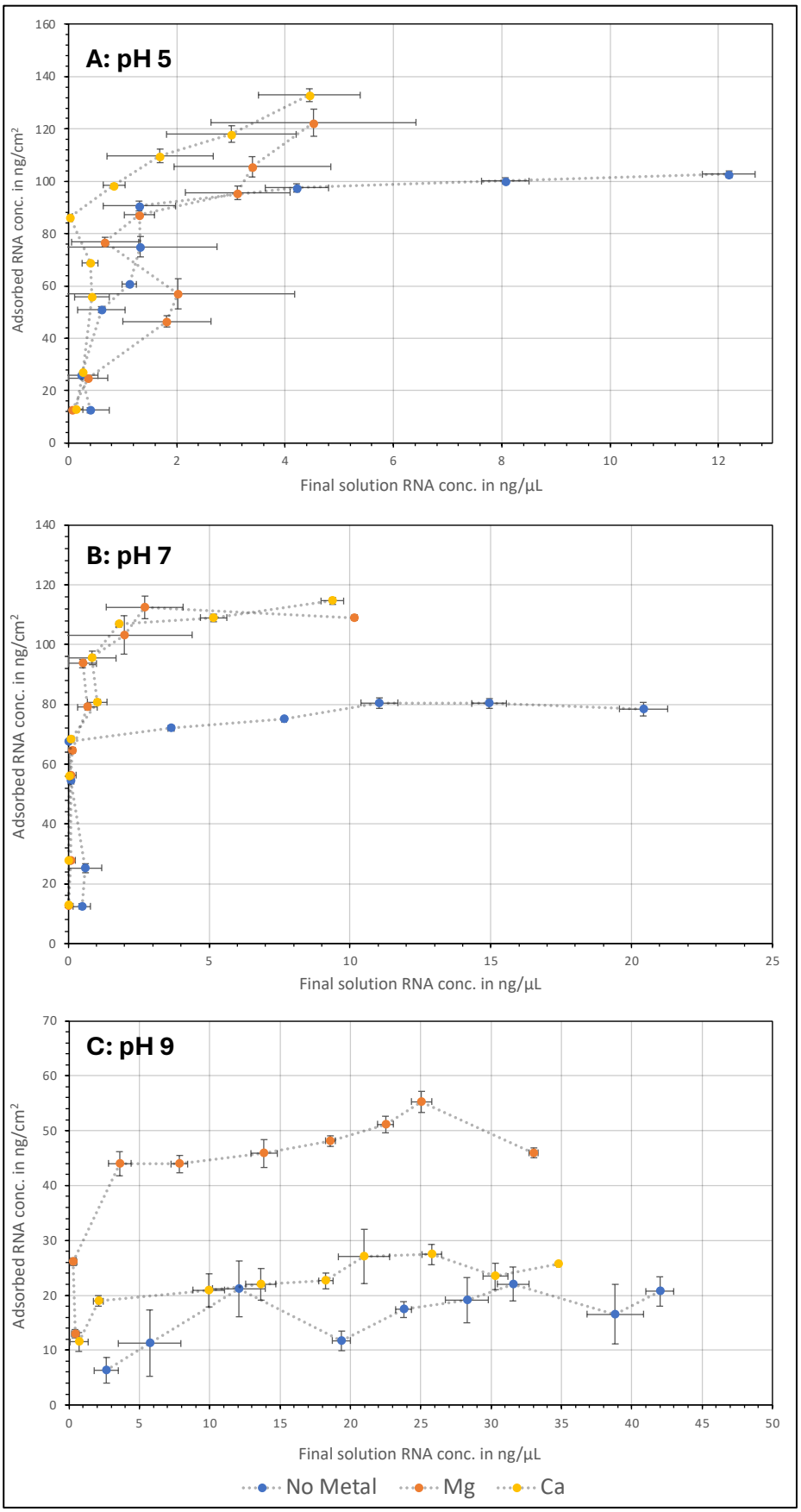


*Figure 10: Concentration dependent RNA adsorption to goethite (1 mg/mL) with $Ca^{2+}$ and $Mg^{2+}$ (200 µM) at the surface at ph 5 (A) (3 mM Acetate, 30 mM NaCl), pH 7 (B) (3 mM HEPES, 30 mM NaCl), and pH 9 (C) (3 mM Sodium Tetraborate, 30 mM NaCl). The pH of the solutions stayed stable during incubation (+- 0.1). The incubation time was 2 h.*

### 3.8 Challenges with new dsRNA batch

After changing to a newly purchased batch of dsRNA, irregularities in concentration measurements could be observed. Concentrations of stock diluted in acetate buffer at pH 5 were 10-15 % less of what was expected when measured on the plate reader and 260/280 ratios were overall higher than in previous measurements. At pH 7 and 9, stock concentrations stayed accurate. To rule out any buffer impurities as a potential cause for these deviations, the buffer was first autoclaved again and additionally a fresh MES buffer (3 mM, 30 mM NaCl) at pH 5 was prepared for comparison. As with both buffers concentrations were still lower than anticipated, the next step was to slowly increase the pH of the same buffer by adding sodium hydroxide to find out whether the concentration anomalies were pH dependent. This was confirmed as above a certain pH value (6.5) measured concentrations started to match expected concentrations again. Absorbance spectra were taken for pH 7 and pH 5 to further investigate this issue (Fig. 11). These spectra showed that the absorbance peak was slightly shifted towards a shorter wavelength for dsRNA diluted in pH 5 buffer. As protein impurities of dsRNA are usually indicated by a 260/280 ratio of less than 2.1 ("Interpretation of nucleic acid 260/280 ratios," 2012), and washing the material in silica spin columns did not cause any significant change in 260/280 ratios at pH 5, these impurities were excluded as a potential cause for concentration issues. Additionally, the 260/280 ratios of measurements with the new batch were overall higher than for the old batch across all pH values. These ratios can be affected by differences in nucleotide composition of the nucleic acids measured (Lehninger, 1975). Uracil and adenine for example tend to have 260/280 ratios of 4.0 and 4.5 respectively ("NanoDrop One User Guide," 2016). As the purchased dsRNA is a poly(A:U) molecule, the question arises whether the 260/280 ratio indicating product purity, should be higher than what was observed, if the material is pure. No further information on potential changes in product production and contents could be obtained from the manufacturer, which is

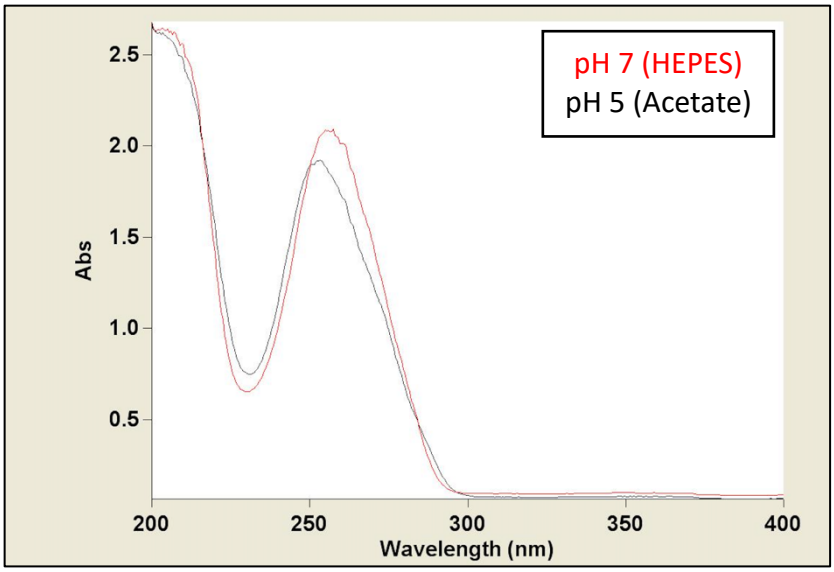


*Figure 11: Light absorbance spectra of 100 ng/µL dsRNA in HEPES (3 mM, 30 mM NaCl, pH 7) and Acetate buffer (3 mM, 30 mM NaC, pH 5).*

why causes can only be speculated on. Further knowledge on the product would be required to propose a hypothesis.

### 3.9 Differences in adsorption data with old and new dsRNA batch

Differences in adsorption behaviour could be observed in an additional trial run with the new dsRNA batch at pH 9 (Fig. 12). The old dsRNA showed significantly higher adsorption to the mineral surface than the new dsRNA batch. This opens up the question of which differences in material could cause differing adsorption behaviour. As 260/280 ratios were higher for the new batch and this ratio can depend on the nucleotide composition of the nucleic acid molecules measured, an altered nucleotide composition in the new batch could be one potential explanation for these differences. If this was the case, it might hint towards nucleotide compositions influencing adsoption behaviour to mineral surfaces. However, due to the lack of information, it can only be speculated.

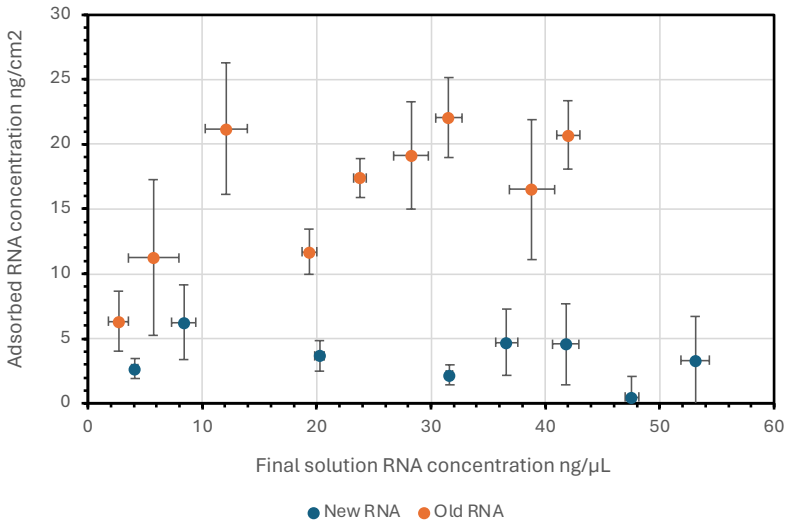


*Figure 12: Concentration dependent adsorption of dsRNA to goethite (1 mg/mL) at pH 9 (3 mM Sodium Tetraborate, 30 mM NaCl) with the old RNA batch (orange) and the new batch (blue). Incubation time was 2 h.*

### 3.10 dsRNA degradation by goethite

Degradation of dsRNA by goethite in the presence of $Ca^{2+}$ and $Mg^{2+}$ was assessed in degradation experiments. Due to issues with concentration measurements of the new dsRNA batch at pH 5, only conditions at pH 7 and 9 were investigated. For the following comparisons of degradation results with the adsorption data from this thesis, it is important to exercise caution. The adsorption experiments were conducted with the original batch of dsRNA, while the degradation experiments utilized the new batch. The difference in materials may influence

the comparability of the results, as variations between the batches could affect the interaction dynamics with the goethite surface. Results form adsorption experiments at pH 9 with the new material deviated from previous experiments with the old batch (Fig. 12). Therefore, any conclusions drawn from these comparisons should be considered with this potential variability in mind.

This whole degradation study was adjusted from Zhang et al. (2023), additionally introducing divalent cations to the system. While Zhang et al. (2023) used agarose gel electrophoresis in combination with image analysis to quantify loss of intact dsRNA, here the TapeStation was used for analysing the extent of degradation. As no screen tapes for dsRNA analysis were available from Agilent, tapes for ssRNA and DNA had to be used instead. As measurements of the same concentration of dsRNA on the TapeStation were inconsistent, concentration ratios had to be used for quantifying degradation.

The extent of degradation was measured on the TapeStation and quantified using equation II (see Appendix, Table A3). Specific size ranges were classified as intact or degraded and ratios of the respective areas under the graph were calculated. Intact dsRNA diluted directly from the stock had a *D*-value of approximately 0.1 (Fig. 13). When the ratio calculated for a specific sample is higher than this value, the dsRNA in the sample is at least partially degraded. The higher *D*, the further degradation has progressed.

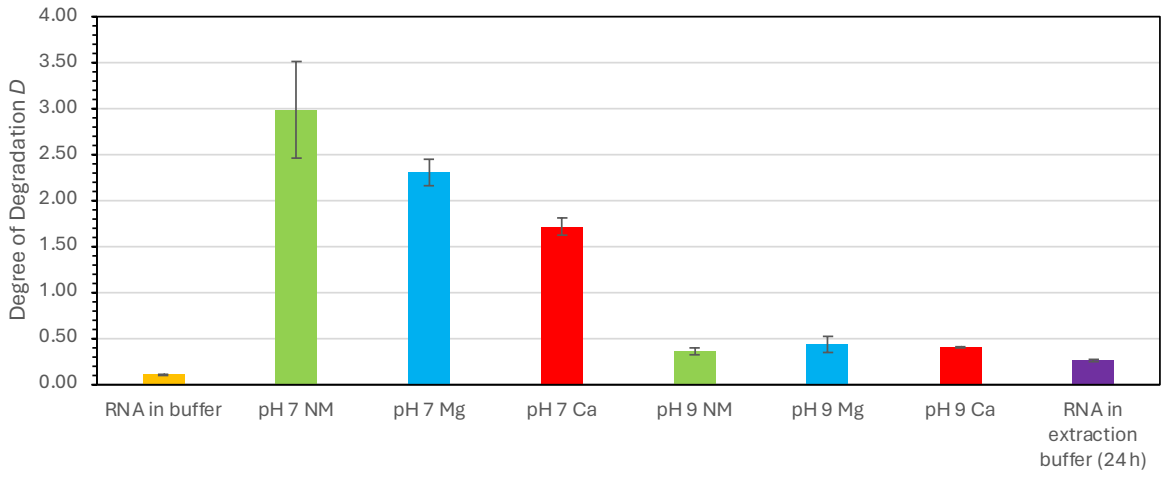


*Figure 13: Degree of Degradation* D *of dsRNA by goethite at pH 7 and 9 with no metal (NM), calcium or magnesium at the surface, calculated using equation II.*

Expectations for the extent of degradation were based on the results of previous adsorption experiments. Hence, at pH 7, $Ca^{2+}$ was expected to enhance degradation more strongly than $Mg^{2+}$, whereas at pH 9, the reverse trend is expected.

Overall, it could be observed that degradation by goethite was much faster at pH 7 (Fig. 15) than at pH 9 (Fig. 14). When no cations were present, the extent of degradation was approximately 10 times as high at pH 7 compared to pH 9 (Fig. 13). These findings align with previous results published on dsRNA degradation by goethite (Zhang et al., 2023). At higher pH, the reduced dsRNA contact with the goethite surface is primarily due to repulsive electrostatic forces between the negatively charged dsRNA molecules and the similarly charged mineral surface. This diminished interaction leads to weaker degradation of dsRNA (Zhang et al., 2023). Although the presence of metal cations may have marginally increased dsRNA degradation at pH 9 relative to the no metal control, the extent of degradation was still significantly below that observed in any condition at pH 7. As diffusion of dsRNA to the goethite surface is not favourable under the conditions at pH 9 due to strong repulsive forces with negative charges at the mineral surface, the presence of divalent metal cations likely enhanced overall contact between the surface and dsRNA by screening charges, resulting in slightly more degradation than when no metal was present. However, differences in degradation between the three treatments were very small (Fig. 13) compared to the significant increase in adsorption, especially with $Mg^{2+}$ . This indicates, that at pH 9, dsRNA seems to be able to adsorb to goethite, without being significantly degraded, and hence could potentially be stabilised at the surface.

At pH 7, degradation was most pronounced when no metals were present at the goethite surface, with magnesium slightly reducing degradation, and calcium providing the most significant protection against degradation (Fig. 13). This observation aligns with results from adsorption data and the hypothesis that calcium forms stronger cation bridges between dsRNA and the mineral surface, preventing degradation to a certain extent, was supported. When dsRNA is adsorbed through these cation bridges rather than through direct inner-sphere complex formation with goethite, the likelihood of hydrolysis is reduced, thereby slowing down the degradation process. However, compared to the intact RNA stock the degradation of all three treatments at pH 7 was relatively far progressed, raising the question of how significant these protective effects from calcium and magnesium are for the fate of dsRNA pesticides in soils.

When looking at the peak shape of degrading dsRNA at pH 7 it can be noted that the overall shape changed, compared to the peak of intact dsRNA at pH 7 (Fig. 15). The peaks of dsRNA degraded by goethite exhibit a sort of tail towards higher fragment legths and molecules seem to be concentrating towards smaller fragments. It looks like there could potentially be a halt or at least a slow-down in degradation rate for smaller sized fragments. This hypothesis can be

supported by the findings from Zhang et al. (2023). When comparing degradation kinetics of 106 bp ssRNA, 1006 bp ssRNA, and 1000 bp dsRNA, degradation was approximately 3-fold slower for dsRNA compared to the 1006 bp ssRNA but even 10-fold slower for the smaller 106 bp ssRNA fragments with an hydrolysis half-life of 70 h. Fragment size thus even excerted a larger effect on degradation rates than the difference between single- and doublestranded molecules. This hints at fragment size being an important parameter for degradation on mineral surfaces. Since dsRNA is more stable than ssRNA, dsRNA molecules with a size of around 100 bp can be expected to degrade even slower than ssRNA of the same size. The question arises, whether degradation of smaller dsRNAs (<100 bp) by goethite is even happening on environmentally relevant time scales, especially considering that some dsRNA pesticides have been reported to belong within this size range (Bolognesi et al., 2012). The small quantities of single nucleotides that could be extracted from goethite surfaces Zhang et al. (2023) after 190 days of incubation further support the relevance of this question.

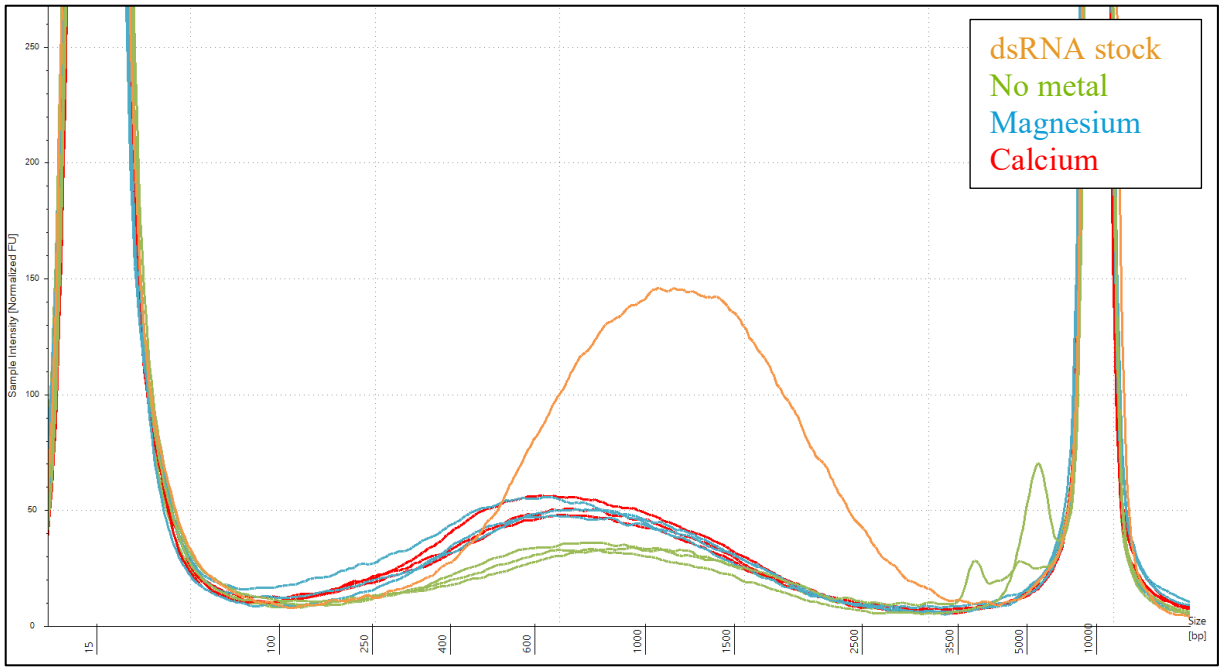


*Figure 14: Fragment size distribution (measured on the TapeStation) of extracted dsRNA incubated with just goethite (1 mg/mL, green), goethite and $Mg^{2+}$ (200 µM, blue), and goethite and $Ca^{2+}$ (200 µM, red) at pH 9 (3 mM Sodium Tetraborate, 30 mM NaCl). Incubation with goethite was 20 h. Extraction time was 24 h in extraction buffer (3 mM Sodium tetraborate, 100 mM NaCl, 12 mM Orthophosphate, pH 9). The orange peak shows the size distribution of intact dsRNA stock at pH 9. Initial experimental dsRNA concentrations were 20 ng/µL.*

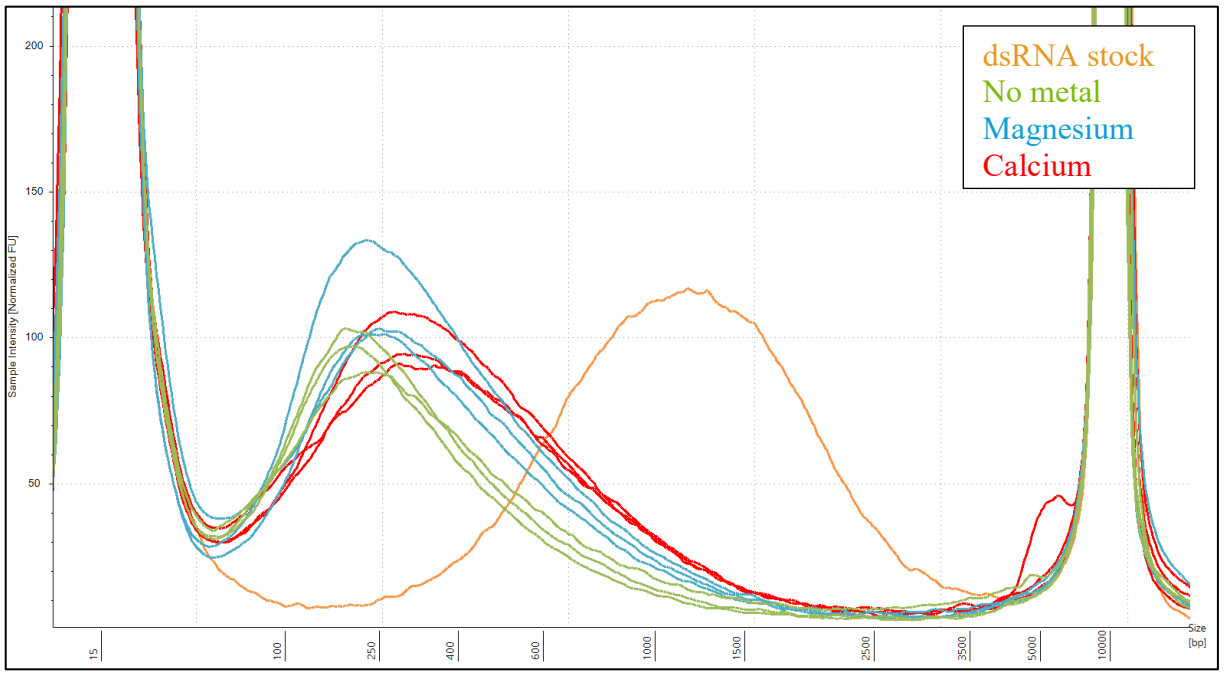


*Figure 15: Fragment size distribution (measured on the TapeStation) of extracted dsRNA incubated with just goethite (1 mg/mL, green), goethite and $Mg^{2+}$ (200 µM, blue), and goethite and $Ca^{2+}$ (200 µM, red) at pH 7 (3 mM HEPES, 30 mM NaCl). Incubation with goethite was 20 h. Extraction time was 24 h in extraction buffer (3 mM Sodium tetraborate, 100 mM NaCl, 12 mM Orthophosphate, pH 9). The orange peak shows the size distribution of intact dsRNA stock at pH 7. Initial experimental dsRNA concentrations were 20 ng/µL.*

Fig. 16 shows that dsRNA was slightly degraded when incubated in extraction buffer over a period of 20 h. This contradicts expectations of dsRNA being stable under extraction buffer conditions. The buffer was adjusted from Zhang et al. (2023) with the only alteration of increasing the pH from 7 to 9. Previous studies have shown, that dsRNA is relatively stable against alkaline hydrolysis at higher pH (Zhang et al., 2021), which makes pH an unlikely driver for the degradation observed. Potentially, RNases were introduced to the system somehow, causing this effect. As all treatments were incubated in extraction buffer for the same amount of time, any degrading effects by the buffer were likely to be the same for all conditions and thus and overall ratios would likely not be affected.

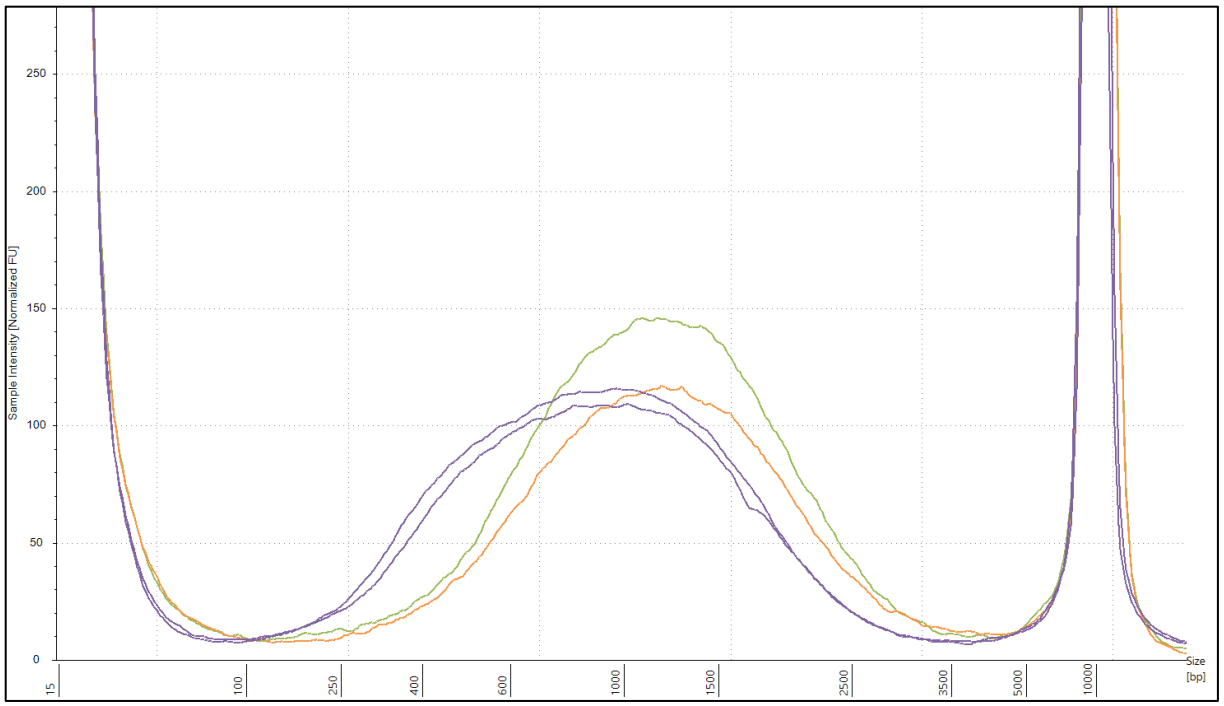


*Figure 16: Size distributions measured on the TapeStation of dsRNA freshly diluted in pH 9 buffer (3 mM Sodium Tetraborate, 30 mM NaCl, green), pH 7 buffer (3 mM HEPES, 30 mM NaCl, orange), and after 24 h in extraction buffer (3 mM Sodium tetraborate, 100 mM NaCl, 12 mM Orthophosphate, pH 9).*

# 4 Conclusion and Environmental Implications

This master thesis assessed the impact of the divalent cations $Mg^{2+}$ and $Ca^{2+}$ on dsRNA hydrolysis at the goethite surface aiming to assess their influence on the stability of novel dsRNA pesticides in soil environments. As expected, goethite facilitates dsRNA hydrolysis, a process that is reflected in the adsorption kinetics data, which contrasts with the adsorption behavior observed with montmorillonite. While both $Ca^{2+}$ and $Mg^{2+}$ increase adsorption of dsRNA to goethite, they decrease the rate of dsRNA degradation by goethite at pH 7, as hypothesized. At pH 9, a slight reversal of this effect was observed, although it was marginal. Calcium, in particular, caused a more significant reduction in dsRNA degradation compared to magnesium at pH 7, likely due to its ability to form inner-sphere complexes. Nevertheless, even though there is a difference in degradation rates caused by the presence of metals, the relevance for the stability of dsRNA in the environment should be discussed. While metal ions at the goethite surface may slow degradation, degradation was still far advanced at neutral pH. The more relevant observation is rather, that at pH 9, degradation rate appears to be low, even with metals at the goethite surface, although these metals significantly increase overall adsorption to goethite. This means, in more alkaline soils, dsRNA molecules could be removed from solution and bound to goethite surfaces without being rapidly degraded, which could reduce transport and bioavailability while increasing stability (Sodnikar et al., 2021).

Smaller fragments of dsRNA were expected to be degraded more slowly at the mineral surface, which is supported by the TapeStation data for pH 7. This raises important questions about whether dsRNA is completely degraded or merely fragmented by goethite on environmentally relevant timescales. This is particularly important given that many dsRNA pesticides are relatively small (Zhang et al., 2023). A second question to be answered in this context is, whether fragmented dsRNA pesticides can still be biologically active, considering they are spliced into 21 bp long fragments within insect cells (Price & Gatehouse, 2008).

Overall, research on dsRNA stability in soils within the last few years implies, that dsRNA seems to degrade in soils rather quickly through both abiotic and biotic degradation pathways at near-neutral pH values (Parker et al., 2019; Zhang et al., 2023; Zhang et al., 2020). However, due to its instability, dsRNA pesticides are often applied to plants using protectants or stabilizers such as liposome encapsulations, EDTA formulations, or formulations with guanylated polymers (Castellanos, Smagghe, Sharma, Oliveira, & Christiaens, 2019;

Christiaens et al., 2018). These additives could potentially influence the stability of dsRNA pesticides in soils as they are designed to make these pesticides more stable for the insect gut. Future research should focus on the implications of specific additives for the environmental risk of dsRNA pesticides.

# 5 References


Aardema, B. W., Lorenz, M. G., & Krumbein, W. E. (1983). Protection of sediment-adsorbed transforming DNA against enzymatic inactivation. *Applied and Environmental Microbiology, 46*(2), 417-420.

Ahmed, W., Angel, N., Edson, J., Bibby, K., Bivins, A., O'Brien, J. W., . . . Li, J. (2020). First confirmed detection of SARS-CoV-2 in untreated wastewater in Australia: a proof of concept for the wastewater surveillance of COVID-19 in the community. *Science of the Total Environment, 728*, 138764.

Antelo, J., Avena, M., Fiol, S., López, R., & Arce, F. (2005). Effects of pH and ionic strength on the adsorption of phosphate and arsenate at the goethite–water interface. *Journal of colloid and interface science, 285*(2), 476-486.

Atouei, M. T., Rahnemaie, R., Kalanpa, E. G., & Davoodi, M. H. (2016). Competitive adsorption of magnesium and calcium with phosphate at the goethite water interface: Kinetics, equilibrium and CD-MUSIC modeling. *Chemical Geology, 437*, 19-29.

Balboa, S., Mauricio-Iglesias, M., Rodriguez, S., Martínez-Lamas, L., Vasallo, F. J., Regueiro, B., & Lema, J. M. (2021). The fate of SARS-COV-2 in WWTPS points out the sludge line as a suitable spot for detection of COVID-19. *Science of the Total Environment, 772*, 145268.

Baum, J. A., Bogaert, T., Clinton, W., Heck, G. R., Feldmann, P., Ilagan, O., . . . Pleau, M. (2007). Control of coleopteran insect pests through RNA interference. *Nature biotechnology, 25*(11), 1322-1326.

Beall, G. W., & Powell, C. E. (2011). *Fundamentals of polymer-clay nanocomposites*: Cambridge University Press.

Beall, G. W., Sowersby, D. S., Roberts, R. D., Robson, M. H., & Lewis, L. K. (2009). Analysis of oligonucleotide DNA binding and sedimentation properties of montmorillonite clay using ultraviolet light spectroscopy. *Biomacromolecules, 10*(1), 105-112.

Berg, J. M., Tymoczko, J. L., Gatto jr, G. J., & Stryer, L. (2018). *Stryer Biochemie* (8th ed. 2018. ed.). Berlin, Heidelberg :: Springer Berlin Heidelberg : Imprint: Springer Spektrum.

Biggs, J., Ewald, N., Valentini, A., Gaboriaud, C., Dejean, T., Griffiths, R. A., . . . Brotherton, P. (2015). Using eDNA to develop a national citizen science-based monitoring programme for the great crested newt (Triturus cristatus). *Biological conservation, 183*, 19-28.

Biopesticides Market Research Report. (2023). Retrieved from https://www.marketsandmarkets.com/Market-Reports/biopesticides-267.html?gad_source=1&gclid=Cj0KCQjwo8S3BhDeARIsAFRmkONJ3DdLkgFA3Ei2_X6yRCqu_ASoC8-SsCcm-0y86h3ZD_ozNrDkfFgaAiAgEALw_wcB

Blum, S. A., Lorenz, M. G., & Wackernagel, W. (1997). Mechanism of retarded DNA degradation and prokaryotic origin of DNases in nonsterile soils. *Systematic and applied microbiology, 20*(4), 513-521.

Blume, H.-P., Brümmer, G. W., Fleige, H., Horn, R., Kandeler, E., Kögel-Knabner, I., . . . Blume, H.-P. (2016). Inorganic soil components—minerals and rocks. *Scheffer/SchachtschabelSoil Science*, 7-53.

Bolognesi, R., Ramaseshadri, P., Anderson, J., Bachman, P., Clinton, W., Flannagan, R., . . . Moar, W. (2012). Characterizing the mechanism of action of double-stranded RNA activity against western corn rootworm (Diabrotica virgifera virgifera LeConte).

Bramlett, M., Plaetinck, G., & Maienfisch, P. (2020). RNA-based biocontrols—a new paradigm in crop protection. *Engineering, 6*(5), 522-527.

Cai, P., Huang, Q., & Zhang, X. (2006). Microcalorimetric studies of the effects of MgCl2 concentrations and pH on the adsorption of DNA on montmorillonite, kaolinite and goethite. *Applied Clay Science, 32*(1-2), 147-152.

Cai, P., Huang, Q., Zhang, X., & Chen, H. (2006). Adsorption of DNA on clay minerals and various colloidal particles from an Alfisol. *Soil Biology and Biochemistry, 38*(3), 471-476.

Cai, P., Huang, Q., Zhu, J., Jiang, D., Zhou, X., Rong, X., & Liang, W. (2007). Effects of low-molecular-weight organic ligands and phosphate on DNA adsorption by soil colloids and minerals. *Colloids and surfaces B: Biointerfaces, 54*(1), 53-59.

Carrado, K. A. (2000). Synthetic organo-and polymer–clays: preparation, characterization, and materials applications. *Applied Clay Science, 17*(1-2), 1-23.

Carretero, M. I. (2002). Clay minerals and their beneficial effects upon human health. A review. *Applied Clay Science, 21*(3-4), 155-163.

Castellanos, N. L., Smagghe, G., Sharma, R., Oliveira, E. E., & Christiaens, O. (2019). Liposome encapsulation and EDTA formulation of dsRNA targeting essential genes increase oral RNAi-caused mortality in the Neotropical stink bug Euschistus heros. *Pest Management Science, 75*(2), 537-548.

Chatterjee, A., Zhang, K., Rao, Y., Sharma, N., Giammar, D. E., & Parker, K. M. (2022). Metal-catalyzed hydrolysis of RNA in aqueous environments. *Environmental Science & Technology, 56*(6), 3564-3574.

Christiaens, O., Tardajos, M. G., Martinez Reyna, Z. L., Dash, M., Dubruel, P., & Smagghe, G. (2018). Increased RNAi efficacy in Spodoptera exigua via the formulation of dsRNA with guanylated polymers. *Frontiers in physiology, 9*, 316.

Collier, A. M., Lyytinen, O. L., Guo, Y. R., Toh, Y., Poranen, M. M., & Tao, Y. J. (2016). Initiation of RNA polymerization and polymerase encapsidation by a small dsRNA virus. *PLoS pathogens, 12*(4), e1005523.

Cristescu, M. E., & Hebert, P. D. (2018). Uses and misuses of environmental DNA in biodiversity science and conservation. *Annual Review of Ecology, Evolution, and Systematics, 49*, 209-230.

Cristiano, E., Hu, Y.-J., Sigfried, M., Kaplan, D., & Nitsche, H. (2011). A comparison of point of zero charge measurement methodology. *Clays and Clay Minerals, 59*(2), 107-115.

Cruz-León, S., Vázquez-Mayagoitia, A., Melchionna, S., Schwierz, N., & Fyta, M. (2018). Coarse-Grained Double-Stranded RNA Model from Quantum-Mechanical Calculations. *The Journal of Physical Chemistry B, 122*(32), 7915-7928. doi:10.1021/acs.jpcb.8b03566

Desa, U. (2019). United Nations Department of economic and social affairs. *Population Division. World Population Prospects*.

Dubelman, S., Fischer, J., Zapata, F., Huizinga, K., Jiang, C., Uffman, J., . . . Carson, D. (2014). Environmental fate of double-stranded RNA in agricultural soils. *PloS one, 9*(3), e93155.

Filipowicz, W. (2005). RNAi: the nuts and bolts of the RISC machine. *Cell, 122*(1), 17-20.

Hannon, G. J. (2002). RNA interference. *nature, 418*(6894), 244-251.

Hazelton, P. A. (2016). *Interpreting soil test results : what do all the numbers mean?* (Third edition. ed.). Clayton, Victoria :: CSIRO Publishing.

Hesselink, F. T. (1977). On the theory of polyelectrolyte adsorption: The effect on adsorption behavior of the electrostatic contribution to the adsorption free energy. *Journal of colloid and interface science, 60*(3), 448-466.

Interpretation of nucleic acid 260/280 ratios. (2012). In *T123 Technical Bulletin. Wilmington, DE, USA: Thermo Scientific*.

Kronberg, B., Holmberg, K., & Lindman, B. (2014). *Surface chemistry of surfactants and polymers*: John Wiley & Sons.

Kurreck, J., Engels, J. W., & Lottspeich, F. (2022). *Bioanalytik*: Springer Spektrum.
Lehninger, A. (1975). Biochemistry the molecular basis of cell structure and function. 2nd edn Worth Publishers. *New York*.
Levy-Booth, D. J., Campbell, R. G., Gulden, R. H., Hart, M. M., Powell, J. R., Klironomos, J. N., . . . Dunfield, K. E. (2007). Cycling of extracellular DNA in the soil environment. *Soil Biology and Biochemistry, 39*(12), 2977-2991.
Lorenz, M. G., & Wackernagel, W. (1987). Adsorption of DNA to sand and variable degradation rates of adsorbed DNA. *Applied and Environmental Microbiology, 53*(12), 2948-2952.
Marshall, N. T., Vanderploeg, H. A., & Chaganti, S. R. (2021). Environmental (e) RNA advances the reliability of eDNA by predicting its age. *Scientific reports, 11*(1), 2769.
Martinez, J., Patkaniowska, A., Urlaub, H., Lührmann, R., & Tuschl, T. (2002). Single-stranded antisense siRNAs guide target RNA cleavage in RNAi. *Cell, 110*(5), 563-574.
Mitter, N., Worrall, E. A., Robinson, K. E., Li, P., Jain, R. G., Taochy, C., . . . Xu, Z. P. (2017). Clay nanosheets for topical delivery of RNAi for sustained protection against plant viruses. *Nature plants, 3*(2), 1-10.
Müller, B., & Sigg, L. (1992). Adsorption of lead (II) on the goethite surface: Voltammetric evaluation of surface complexation parameters. *Journal of colloid and interface science, 148*(2), 517-532.
NanoDrop One User Guide. (2016). Retrieved from https://tools.thermofisher.com/content/sfs/manuals/3091-NanoDrop-One-Help-UG-en.pdf
Nguyen, T. H., & Chen, K. L. (2007). Role of divalent cations in plasmid DNA adsorption to natural organic matter-coated silica surface. *Environmental Science & Technology, 41*(15), 5370-5375.
Nguyen, T. H., Chen, K. L., & Elimelech, M. (2010). Adsorption kinetics and reversibility of linear plasmid DNA on silica surfaces: influence of alkaline earth and transition metal ions. *Biomacromolecules, 11*(5), 1225-1230.
Nicholson, A. W. (1996). Structure, Reactivity, and Biology of Double-Stranded RNA. In W. E. Cohn & K. Moldave (Eds.), *Progress in Nucleic Acid Research and Molecular Biology* (Vol. 52, pp. 1-65): Academic Press.
Nwokeoji, A. O., Kilby, P. M., Portwood, D. E., & Dickman, M. J. (2017). Accurate quantification of nucleic acids using hypochromicity measurements in conjunction with UV spectrophotometry. *Analytical chemistry, 89*(24), 13567-13574.
Obbard, D. J., Gordon, K. H., Buck, A. H., & Jiggins, F. M. (2009). The evolution of RNAi as a defence against viruses and transposable elements. *Philosophical Transactions of the Royal Society B: Biological Sciences, 364*(1513), 99-115.
Ogram, A. V., Mathot, M. L., Harsh, J. B., Boyle, J., & Pettigrew Jr, C. A. (1994). Effects of DNA polymer length on its adsorption to soils. *Applied and Environmental Microbiology, 60*(2), 393-396.
Olds, B. P., Jerde, C. L., Renshaw, M. A., Li, Y., Evans, N. T., Turner, C. R., . . . Shirey, P. D. (2016). Estimating species richness using environmental DNA. *Ecology and evolution, 6*(12), 4214-4226.
Olson, S. (2015). An analysis of the biopesticide market now and where it is going. *Outlooks on pest management, 26*(5), 203-206.
Paget, E., Monrozier, L. J., & Simonet, P. (1992). Adsorption of DNA on clay minerals: protection against DNaseI and influence on gene transfer. *FEMS Microbiology Letters, 97*(1-2), 31-39. doi:10.1111/j.1574-6968.1992.tb05435.x
Parker, K. M., Barragán Borrero, V., Van Leeuwen, D. M., Lever, M. A., Mateescu, B., & Sander, M. (2019). Environmental fate of RNA interference pesticides: adsorption and

degradation of double-stranded RNA molecules in agricultural soils. *Environmental Science & Technology, 53*(6), 3027-3036.
Parker, K. M., & Sander, M. (2017). Environmental fate of insecticidal plant-incorporated protectants from genetically modified crops: knowledge gaps and research opportunities. In: ACS Publications.
Price, D. R., & Gatehouse, J. A. (2008). RNAi-mediated crop protection against insects. *Trends in biotechnology, 26*(7), 393-400.
Pruvost, M., Schwarz, R., Correia, V. B., Champlot, S., Braguier, S., Morel, N., . . . Geigl, E.-M. (2007). Freshly excavated fossil bones are best for amplification of ancient DNA. *Proceedings of the National Academy of Sciences, 104*(3), 739-744.
Romanowski, G., Lorenz, M. G., & Wackernagel, W. (1991). Adsorption of plasmid DNA to mineral surfaces and protection against DNase I. *Applied and Environmental Microbiology, 57*(4), 1057-1061.
Saeki, K., & Kunito, T. (2010). Adsorptions of DNA molecules by soils and variable-charged soil constituents. *Curr. Res. Technol. Educ. Top. Appl. Microbiol. Microb. Biotechnol, 1*, 188-195.
Schmidt, M. P., & Martinez, C. E. (2017). Ironing out genes in the environment: an experimental study of the DNA–goethite interface. *Langmuir, 33*(34), 8525-8532.
Schwertmann, U., & Cornell, R. M. (2000). *Iron oxides in the laboratory: preparation and characterization*: John Wiley & Sons.
Sodnikar, K., Parker, K. M., Stump, S. R., ThomasArrigo, L. K., & Sander, M. (2021). Adsorption of double-stranded ribonucleic acids (dsRNA) to iron (oxyhydr-) oxide surfaces: comparative analysis of model dsRNA molecules and deoxyribonucleic acids (DNA). *Environmental Science: Processes & Impacts, 23*(4), 605-620.
Terada, E., Samoshina, Y., Nylander, T., & Lindman, B. (2004). Adsorption of cationic cellulose derivative/anionic surfactant complexes onto solid surfaces. II. Hydrophobized silica surfaces. *Langmuir, 20*(16), 6692-6701.
Thomsen, P. F., & Willerslev, E. (2015). Environmental DNA–An emerging tool in conservation for monitoring past and present biodiversity. *Biological conservation, 183*, 4-18.
V'kovski, P., Kratzel, A., Steiner, S., Stalder, H., & Thiel, V. (2021). Coronavirus biology and replication: implications for SARS-CoV-2. *Nature Reviews Microbiology, 19*(3), 155-170. doi:10.1038/s41579-020-00468-6
Wilfinger, W. W., Mackey, K., & Chomczynski, P. (1997). Effect of pH and ionic strength on the spectrophotometric assessment of nucleic acid purity. *Biotechniques, 22*(3), 474-481.
Willerslev, E., & Cooper, A. (2005). Ancient dna. *Proceedings of the Royal Society B: Biological Sciences, 272*(1558), 3-16.
Willerslev, E., Hansen, A. J., & Poinar, H. N. (2004). Isolation of nucleic acids and cultures from fossil ice and permafrost. *Trends in Ecology & Evolution, 19*(3), 141-147.
Wood, S. A., Biessy, L., Latchford, J. L., Zaiko, A., von Ammon, U., Audrezet, F., . . . Pochon, X. (2020). Release and degradation of environmental DNA and RNA in a marine system. *Science of the Total Environment, 704*, 135314.
Xu, C.-y., Deng, K.-y., Li, J.-y., & Xu, R.-k. (2015). Impact of environmental conditions on aggregation kinetics of hematite and goethite nanoparticles. *Journal of Nanoparticle Research, 17*, 1-13.
Yates, M. C., Derry, A. M., & Cristescu, M. E. (2021). Environmental RNA: a revolution in ecological resolution? *Trends in Ecology & Evolution, 36*(7), 601-609.
Yu, W. H., Li, N., Tong, D. S., Zhou, C. H., Lin, C. X. C., & Xu, C. Y. (2013). Adsorption of proteins and nucleic acids on clay minerals and their interactions: A review. *Applied Clay Science, 80*, 443-452.

Zhang, K., Ho, K.-P., Chatterjee, A., Park, G., Li, Z., Catalano, J. G., & Parker, K. M. (2023). RNA Hydrolysis at Mineral–Water Interfaces. *Environmental Science & Technology, 57*(22), 8280-8288.

Zhang, K., Hodge, J., Chatterjee, A., Moon, T. S., & Parker, K. M. (2021). Duplex structure of double-stranded RNA provides stability against hydrolysis relative to single-stranded RNA. *Environmental Science & Technology, 55*(12), 8045-8053.

Zhang, K., Wei, J., Huff Hartz, K. E., Lydy, M. J., Moon, T. S., Sander, M., & Parker, K. M. (2020). Analysis of RNA interference (RNAi) biopesticides: Double-stranded RNA (dsRNA) extraction from agricultural soils and quantification by RT-qPCR. *Environmental Science & Technology, 54*(8), 4893-4902.

# 6 Appendix

## 6.1 Goethite RNA kinetics trial runs

50 ng/µL RNA, 2 mg/mL Goethite

- Goethite suspension: 4 mg/mL, hydrated in MQ for 24 h on magnetic stir plate (300 rpm)
- Timepoints: 0, 5, 10, 30 min, 1, 2, 4, 6 h
- 3 reactors (2 mL volume in 5 mL LoBind tubes)
- RNA solution: 100 ng/µL in BisTris buffer (6 mM, 60 mM NaCl)
- In reactors: 50 ng/µL RNA, 30 mM NaCl, 3 mM BisTris, 2 mg/mL Goethite
- Goethite suspension ultrasonicated for 3 min right before mixing of RNA and Goethite
- Aliquots of 100 µL taken out for each timepoint, centrifuged for 20 mins at 20 000 rcf and measured on plate reader
- pH measured after experiment
- goethite suspension pipetted while stirring at 900 rpm
- Shaker setting: C2, 20 rpm

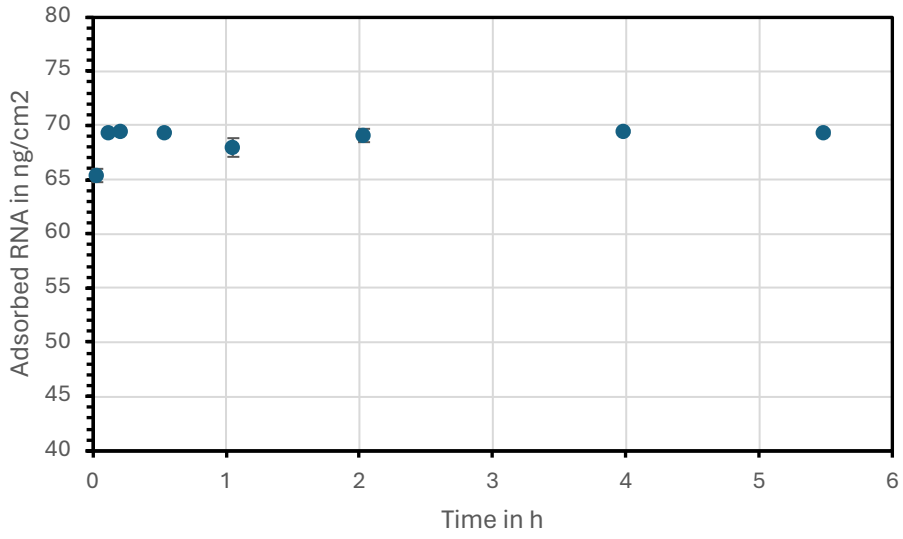


*Figure A1: dsRNA adsorption kinetics to goethite (2 mg/mL) at pH 7 in 3 mM BisTris buffer (30 mM NaCl). Initial dsRNA concentration was 50 ng/µL*

100 ng/µL RNA, 2 mg/mL Goethite

- Timepoints: 0, 5, 20, 30 min, 1, 2, 4, 6, 24 h
- Otherwise, same methods as before

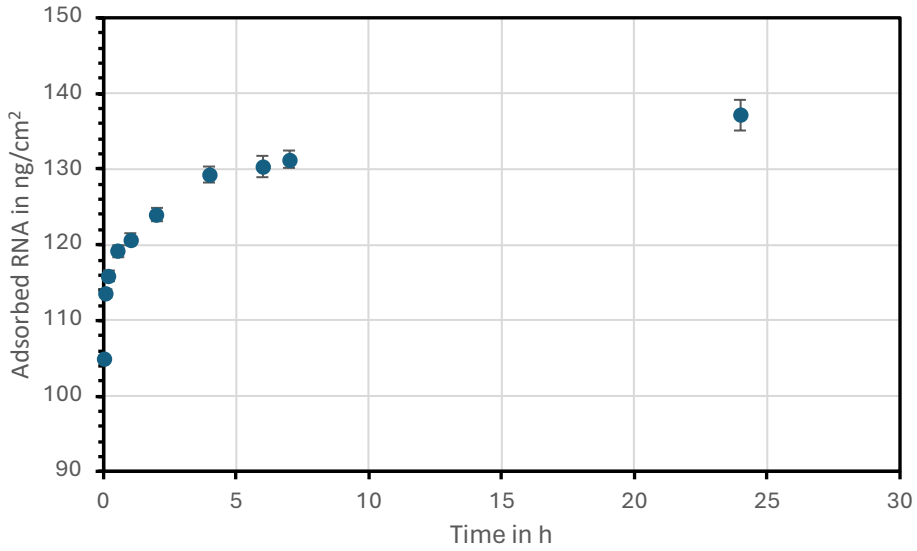


*Figure A2: dsRNA adsorption kinetics to goethite (2 mg/mL) at pH 7 in 3 mM BisTris buffer (30 mM NaCl). Initial dsRNA concentration was 100 ng/µL*

### 6.2 Montmorillonite kinetics trial runs and interference check

Montmorillonite interference check

- Different concentrations of Montmorillonite (10, 8, 4, 2 mg/mL) hydrated in HEPES buffer (3 mM, 30 mM NaCl) over night
- Measured against blank (buffer) on plate reader after centrifuging mineral for 40 mins at 20200 rcf, pipetted straight from supernatant onto plate reader
- For 2 mg/mL supernatant was also taken off right after centrifuging and put into fresh Eppendorf tube

→ when put into fresh tube right away, interference can be prevented

→ Also repeated with 10 mg/mL and 4 mg/mL Montmorillonite (supernatant put in fresh tube right after centrifuging) → same results → Interference can be avoided

*Table A1: Interference in plate reader measurements caused by montmorillonite when sample was directly taken from supernatant in contact with pellet and when supernatant was separated from the pellet right after centrifugation*

| | **2 mg Montmorillonite/mL** | **2 mg Montmorillonite/mL - supernatant separated -** |
|---|---|---|
| | **Interference in ng RNA/µL** | **Interference in ng RNA/µL** |
| | 4.4 | 0 |
| | 2.4 | 0.5 |
| | 7.3 | 0.6 |
| | 6.9 | 0 |
| | 5.2 | 0.1 |
| | 11.5 | 0.3 |
| Average | **6.28** | **0.25** |
| SD | **2.84** | **0.24** |

Montmorillonite and RNA/DNA kinetics Trial Run

- Clay concentration: 4 mg/mL and 10 mg/mL
- RNA and DNA: 50 ng/µL
- Buffer HEPES (3 mM, 30 mM NaCl
- Mineral suspension ultrasonicated for 3 min prior to use
- Reactor volume: 2 mL
- 4 reactors:
    - RNA + 4 mg/mL Montmorillonite
    - RNA + 10 mg/mL Montmorillonite
    - DNA + 4 mg/mL Montmorillonite
    - DNA + 10 mg/mL Montmorillonite
- 2 controls: RNA + buffer, DNA + buffer
- Timepoints: 0, 5, 10, 30 min, 1, 2 h
- pH measured before and after experiment

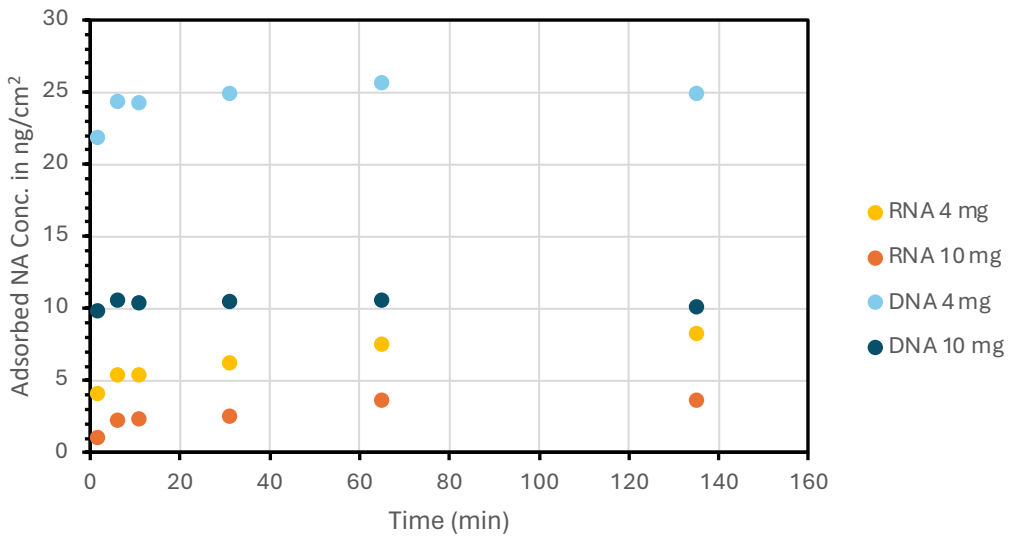


*Figure A3: dsRNA and DNA adsorption kinetics to 4 mg/mL and 10 mg/mL montmorillonite at pH 7 in 3 mM HEPES buffer (30 mM NaCl). Initial nucleic acid (NA) concentration was 50 ng/µL.*

## 6.3 Overview for dsRNA adsorption experiment to a metal loaded goethite surface

*Table A2: Different treatment conditions for RNA adsorption experiments to goethite with respective pH, metal, and RNA concentration.*

| | **Goethite with Mg** | | | **Goethite with Ca** | | | **Goethite with no metal** | | |
|---|---|---|---|---|---|---|---|---|---|
| **5 ng/µL RNA** | Mg 5.5 | Mg 5.7 | Mg 5.9 | Ca 5.5 | Ca 5.7 | Ca 5.9 | NM 5.5 | NM 5.7 | NM 5.9 |
| **10 ng/µL RNA** | Mg 10.5 | Mg 10.7 | Mg 10.9 | Ca 10.5 | Ca 10.7 | Ca 10.9 | NM 10.5 | NM 10.7 | NM 10.9 |
| **20 ng/µL RNA** | Mg 20.5 | Mg 20.7 | Mg 20.9 | Ca 20.5 | Ca 20.7 | Ca 20.9 | NM 20.5 | NM 20.7 | NM 20.9 |
| **25 ng/µL RNA** | Mg 25.5 | Mg 25.7 | Mg 25.9 | Ca 25.5 | Ca 25.7 | Ca 25.9 | NM 25.5 | NM 25.7 | NM 25.9 |
| **30 ng/µL RNA** | Mg 30.5 | Mg 30.7 | Mg 30.9 | Ca 30.5 | Ca 30.7 | Ca 30.9 | NM 30.5 | NM 30.7 | NM 30.9 |
| **35 ng/µL RNA** | Mg 35.5 | Mg 35.7 | Mg 35.9 | Ca 35.5 | Ca 35.7 | Ca 35.9 | NM 35.5 | NM 35.7 | NM 35.9 |
| **40 ng/µL RNA** | Mg 40.5 | Mg 40.7 | Mg 40.9 | Ca 40.5 | Ca 40.7 | Ca 40.9 | NM 40.5 | NM 40.7 | NM 40.9 |
| **45 ng/µL RNA** | Mg 45.5 | Mg 45.7 | Mg 45.9 | Ca 45.5 | Ca 45.7 | Ca 45.9 | NM 45.5 | NM 45.7 | NM 45.9 |
| **50 ng/µL RNA** | Mg 50.5 | Mg 50.7 | Mg 50.9 | Ca 50.5 | Ca 50.7 | Ca 50.9 | NM 50.5 | NM 50.7 | NM 50.9 |
| | **pH 5** | **pH 7** | **pH 9** | **pH 5** | **pH 7** | **pH 9** | **pH 5** | **pH 7** | **pH 9** |

## 6.4 dsRNA degradation by goethite

*Table A3: Degree of dsRNA degradation (D) by goethite at pH 7 and 9 with no metals (NM), calcium, and magnesium at the mineral surface, calculated using equation II.*

| | RNA in buffer | pH 7 NM | pH 7 Mg | pH 7 Ca | pH 9 NM | pH 9 Mg | pH 9 Ca | RNA in extraction buffer (24 h) |
|---|---|---|---|---|---|---|---|---|
| | 0.108 | 2.40 | 2.30 | 1.66 | 0.398 | 0.389 | 0.413 | 0.252 |
| | 0.103 | 3.19 | 2.45 | 1.66 | 0.334 | 0.531 | 0.399 | 0.267 |
| | | 3.39 | 2.16 | 1.83 | 0.336 | 0.386 | 0.409 | |
| Average | 0.105 | 2.99 | 2.31 | 1.71 | 0.356 | 0.435 | 0.407 | 0.260 |
| SD | | 0.524 | 0.146 | 0.097 | 0.036 | 0.083 | 0.007 | |